Physics – Uspekhi **68** (3) 261 – 277 (2025)

PHYSICS OF OUR DAYS

PACS numbers: 05.20.Dd, 05.70.Ln, **51.10.+y**

Nonclassical transport in nonequilibrium rarefied gas flows

V.V. Aristov, S.A. Zabelok, A.A. Frolova

DOI: https://doi.org/10.3367/UFNe.2024.08.039730

Contents

1. Introduction **261**
2. Kinetic approach and possibility of nonclassical transport **263**
2.1 Boltzmann equation; 2.2 Phenomenological momentum and heat transfer laws; 2.3 Example of anomalous relation between heat flux and temperature gradient
3. Heat transfer in classical and nonclassical cases **264**
3.1 Classical heat transfer problem; 3.2 Heat transfer problem with nonequilibrium reflection
4. Nonequilibrium flow with nonuniform relaxation **267**
4.1 Nonuniform relaxation in supersonic regime throughout flow region; 4.2 Nonuniform relaxation in complex regimes
5. Identifying anomalous transfer in flow past bodies **270**
6. Study of anomalous transport in flows with 'membrane-type' boundary conditions **271**
7. Consistency with second law of thermodynamics, nonequilibrium entropy, and prospects for experimental verification **274**
8. Conclusions **276**
References **276**

Abstract. We discuss physical phenomena in nonequilibrium gas flows where the classical Stokes and Fourier laws for stress and heat transfer are violated. Fundamental differences are revealed between the kinetic description and methods of the thermodynamics of nonequilibrium processes. We study classes of problems for nonequilibrium rarefied gas flows with nonclassical transport. Prospects of experimental verification of the effects are also discussed.

Keywords: kinetic theory, Boltzmann equation, nonequilibrium flows, nonclassical transport processes

1. Introduction

The study of highly nonequilibrium gas flows is currently becoming increasingly important (see, e.g., [1, 2]). This is due to the development of laser technology, the study of the upper atmosphere and the interstellar space and plasma, the development of nanotechnology, and the study of processes in micro- and nano-electromechanical systems, i.e., processes occurring on the scale of characteristic distances from several to hundreds of micrometers. Moreover, the Navier–Stokes (NS) equations, typically used in traditional gasdynamic problems, may not give correct results in this case, because they are derived in the framework defined by the Newtonian paradigm, the continuum model, and thermodynamic equilibrium.

The assumption of thermodynamic equilibrium means that the collisions of molecules occur frequently enough over a short time interval, while the parameters of the gas change little over distances comparable to the mean free path l_0, which corresponds to a small Knudsen number Kn (equal to the ratio of l_0 to the characteristic scale L of the flow).

The formulation of the NS equations involves fundamental assumptions about linear relations between the stress tensor and the flow deformation rate tensor (Newton's viscosity law), as well as between the heat flux and the temperature gradient (Fourier's law); the condition of the absence of slip and temperature jump on the surface of bodies is traditionally accepted as boundary conditions. Because the NS equations do not give a correct picture of strongly nonequilibrium gas flows, nonphenomenological connections to transport theory and new phenomena can be discovered in the framework of the kinetic approach based on the Boltzmann equation (BE). Finding new areas of application of the kinetic approach should be accompanied by positioning this theory between the macroscopic description with the Euler or NS equations and the atomic–molecular description with the Newton or Schrödinger equations.

To emphasize the specificity of kinetic methods, it is worth quoting Grad [3], who is one of the most famous authors in the field of kinetic theory, regarding the special role of the BE among the equations of mathematical physics: "... The usual thermodynamics of irreversible processes deals with small (linear) deviations from equilibrium, while the Boltzmann

V.V. Aristov [(a)], **S.A. Zabelok** [(b)], **A.A. Frolova** [(c)]
Federal Research Center Computer Science and Control of the Russian Academy of Sciences,
ul. Vavilova 44, korp. 2, 119333 Moscow, Russian Federation
E-mail: [(a)] aristovvl@yandex.ru, [(b)] s.zabelok@yandex.ru, [(c)] aafrolova@yandex.ru

Received 16 April 2024, revised 12 July 2024
Uspekhi Fizicheskikh Nauk **195** (3) 276 – 293 (2025)
Translated by S Alekseev

equation allows for large (nonlinear) deviations. ... It is necessary to rigorously distinguish between the nonlinearity of the hydrodynamic equations and the linearity of the irreversibility mechanism. The fundamental advantage of the Boltzmann equation is that it allows one to describe significant changes in the gas flow properties over the mean free path....''

For a long time, violations of the Fourier (or Stokes) law were not detected when solving various problems of rarefied gas dynamics, because the main interest was to determine the behavior of macroparameters in nearly continuous flow regimes, where the effect of anomalous transfer is either expressed weakly or suppressed altogether.

However, when studying gas flows in micro- and nanogeometry, interesting phenomena are discovered that are not observed in the continuum regime. For example, the flow rate of a gas moving at a given pressure drop in a channel reaches a minimum at the Knudsen number $\mathrm{Kn} \sim 1$; this phenomenon is called the Knudsen paradox [4]. Another unique phenomenon discovered in rarefied flow regimes is the process of thermal slip of gas caused by nonuniform heating of the channel walls. This process is currently used to create Knudsen pumps, a new generation of compressors without moving parts. Knudsen pumps are based on the phenomenon of thermal transpiration, which has been known for a long time [5–7] but was not immediately recognized, because the connection between this phenomenon and actual applications was unclear. From the standpoint of classical hydrodynamics, there is no steady flow induced only by the temperature field without external forces such as gravity and pressure. In a rarefied gas, the temperature field plays a significant role in creating a gas flow that is independent of time [8]. In [9], various types of thermally induced flows are presented and an extensive review of recent research on this topic is given. The important role played by kinetic effects in the study of evaporation, condensation, and heat transfer processes is demonstrated in [10].

As a result of developing microtechnologies, advances in studying the properties of new materials, and the improvement of numerical methods, we are witnessing progress in the study of highly nonequilibrium flows. For example, for some stationary rarefied gas flows, it was deduced from the BE that, on scales of the order of the mean free path, the dissipative flows (of the heat flux and viscous stress tensor) can depend on the derivatives of the velocity and temperature in a way that is fundamentally different from the classical Newton and Fourier prescriptions, especially if the process involves zones of highly nonequilibrium flow supported by some nonequilibrium conditions at the flow region boundaries. At the macroscopic level, the relations between dissipative flows and the derivatives of the corresponding quantities remain linear, but, in contrast to the classical formulations, they can involve positive, rather than negative, proportionality coefficients, which drastically changes the physical picture of the process, because heat is then transferred from a cold region to a hot one, and momentum is transferred in the direction of increasing velocity. The aim of this paper is to identify such effects in various flows.

However, violations of classical transport laws can also occur in flows with equilibrium boundary conditions. For example, in the problem of the shock wave structure at high Mach numbers ($\mathrm{M} > 8$) [11–14], nonmonotonic behavior of temperature was noted (based on the Mott–Smith approximation for the solution) at a constant sign of the heat flux. This effect (discovered in the 1970s in solving the BE) was questioned by researchers due to the low accuracy of the numerical methods used. Confirmation was obtained much later using reliable numerical approaches: a conservative solution of the BE and, independently, the direct statistical modeling (DSMC) method (see, e.g., [15]).

Nonclassical heat transfer effects were also discovered in the study of Poiseuille flows in [16, 17]. In some relatively recent studies (see, e.g., [18, 19]), the possibility of anomalous heat transfer has also been confirmed. A theoretical analysis is presented in [18], and a numerical solution of the problem of flow in a rectangular cavity caused by the motion of the upper wall (cover) is presented in [19].

Local heat transfer anomalies have been found in classical formulations of problems for Poiseuille, Couette, Reynolds, and other flows with equilibrium boundary conditions [20–22]. For example, in [22], a Reynolds flow problem is considered in which a minimum of transverse temperature is observed on the axis, while the sign of the heat flux in the transverse direction does not change, causing anomalous heat transfer near the axis.

The identification of new transfer effects in various flows gives rise to new problems. Nonlinear non-Fourier heat transfer replacing the usual linear transfer in accordance with the Fourier law is considered in [23–25], where extended thermodynamics are also discussed. Previously, the presence of a longitudinal heat flux in a rarefied gas for the Couette problem at zero temperature gradient was discovered in a number of studies [26].

We also note studies (see, e.g., [27]) of the flows at small Knudsen numbers, where the Burnett terms of the expansion exceed the NS terms under certain physical conditions, which introduces additional nonlinear terms into Newton's law. Stresses arise due to the temperature and concentration nonuniformity.

The relation between kinetic theory and nonequilibrium thermodynamics is reviewed in detail in [28]. It is noted there, inter alia, that some researchers, including Grad, proposed a generalization of the methods of nonequilibrium thermodynamics to the case where the nonequilibrium state of a gas (and entropy) are determined not only by local values of the thermodynamic variables (density, internal energy, and component concentrations), but also by an arbitrary number of additional state variables (moments of the distribution function). When such a generalization is developed further, additional terms appear in the expression for entropy production (which is part of the entropy balance equation) that contain higher-order coordinate derivatives of the fundamental thermodynamic variables and velocity (order higher than one). The system of phenomenological equations for flows and forces has been extended accordingly [29–30]. But, in contrast to kinetic theory, a macroscopic approach is essentially used there (see, e.g., relatively recent study [31]). The fundamental difference between the description's of entropy in kinetics and the thermodynamics of irreversible processes was noted in [14].

Generalizations of Fourier's and Newton's laws to systems with long relaxation times have been derived in the framework of extended thermodynamics of irreversible processes [32, 33]. The crux of this formalism is the hypothesis that dissipative flows (of heat and the viscous stress tensor) are included in the set of basic independent entropy variables, which allowed obtaining evolution equations for these flows. This approach is especially useful in

studying the thermodynamics of nonequilibrium steady states and systems with long relaxation times, such as viscoelastic media or systems at low temperatures (also see [34–35]).

We note that nonequilibrium conditions at the boundaries of a gas flow do not always give rise to anomalous transfer processes, and therefore, when studying processes in micro- and nanoscale devices, it is of interest to describe the conditions for such flows. In this paper, we demonstrate the occurrence of anomalous transfer effects in flows with nonequilibrium boundary conditions. For preliminary estimates, a theoretical analysis is used, but the main research tool is numerical modeling with the Unified Flow Solver (UFS) software package [36], which is based of methods for directly solving the BE. Prospects for experimental verification of the detected effects are also discussed.

2. Kinetic approach and possibility of nonclassical transport

2.1 Boltzmann equation

The basis of the kinetic theory is the BE for the evolution of the distribution function (DF) of the velocities of monatomic molecules, $f(\mathbf{r}, \boldsymbol{\xi}, t)$. For a single-component gas, the equation has the form

$$\frac{\partial f}{\partial t} + \boldsymbol{\xi}\,\nabla_r f + \frac{\mathbf{F}}{m}\,\nabla_\xi f = I(f,f)\,, \tag{1}$$

where $\mathbf{r} = (x, y, z)$ is the coordinate vector in physical space, $\boldsymbol{\xi} = (\xi_x, \xi_y, \xi_z)$ is the velocity vector, t is the time, $\mathbf{F}$ is the vector of force, and m is the mass of a molecule. The term with the external force is omitted in what follows, because we are interested in flows not affected by external fields. In the case of binary collisions, the collision integral $I(f,f)$ is an integral operator local in physical space,

$$I(\boldsymbol{\xi}) = \int_{S^2} \mathrm{d}\omega \int_{R^3} \bigl(f(\boldsymbol{\xi}_1')f(\boldsymbol{\xi}') - f(\boldsymbol{\xi}_1)f(\boldsymbol{\xi})\bigr)|\mathbf{g}|\sigma(g,\chi)\,\mathrm{d}\boldsymbol{\xi}_1\,,$$

where $\mathbf{g} = \boldsymbol{\xi}_1 - \boldsymbol{\xi}$ is the relative velocity vector of colliding particles, $\mathrm{d}\omega$ is the solid angle, $\sigma(g,\chi)$ is the differential collision cross section, χ is the scattering angle depending on the potential of the interparticle interaction field, and $\boldsymbol{\xi}'$ and $\boldsymbol{\xi}_1'$ are the particle velocities after the collision.

In kinetic theory, macroscopic variables such as the particle number density n, the mean velocity $\mathbf{u}$, the temperature T, the H-function, the heat flux vector $\mathbf{q}$, and the stress tensor $\mathbf{P}$ are given by averaging the DF over the velocity space with appropriate weights,

$$(n, m\mathbf{u}, 3k_\mathrm{B}nT, H, \mathbf{q}, \mathbf{P}) = \int \left(1, \boldsymbol{\xi}, mC^2, \ln(f), \frac{m\mathbf{C}C^2}{2}, m\mathbf{C}\otimes\mathbf{C}\right) f\,\mathrm{d}\boldsymbol{\xi}\,, \tag{2}$$

while the pressure p and the viscous stress tensor $\mathbf{p}$ are given by $p = nk_\mathrm{B}T$ and $\mathbf{p} = \mathbf{P} - p\mathbf{I}$, where k_B is the Boltzmann constant.

Along with the exact BE, model relaxation equations are used in numerical modeling and in obtaining approximate solutions and estimates:

$$\frac{\partial f}{\partial t} + \boldsymbol{\xi}\nabla_r f = \nu(F^+ - f)\,. \tag{3}$$

In the case of the Shakhov model (the S-model equation) [37],

$$F^+ = F_\mathrm{M}(n,\mathbf{u},T)\left[1 + \frac{2m}{5pk_\mathrm{B}T}\,(1-\mathrm{Pr})\,\mathbf{q}\,\mathbf{C}\left(\frac{mC^2}{2k_\mathrm{B}T} - \frac{5}{2}\right)\right],$$

where $F_\mathrm{M}(n,\mathbf{u},T) = n\,(m/(2\pi k_\mathrm{B}T))^{3/2}\exp(-mC^2/2k_\mathrm{B}T)$ is the Maxwell function, Pr is the Prandtl number, $\mathbf{C} = \boldsymbol{\xi} - \mathbf{u}$ is the relative molecular velocity vector, and $\nu = p/\mu$ is the collision rate, which depends on the viscosity coefficient μ and pressure p. For $\mathrm{Pr} = 1$, Eqn (3) reduces to the well-known BGK relaxation equation [38].

When solving kinetic equations, dimensionless quantities are typically used, normalized to the characteristic parameters of the process such as the length scale L, the temperature T_ref, the particle number density n_ref and mass m, and the most probable molecular velocity $u_\mathrm{T} = \sqrt{2k_\mathrm{B}T_\mathrm{ref}/m}$. The introduction of characteristic quantities leads to the appearance of a rarefaction parameter on the right-hand side of the equation: this is the Knudsen number $\mathrm{Kn} = l_0/L$, where l_0 is the mean free path, which, in the case of the hard-sphere model of particle interaction, is determined by the molecular diameter d and the particle number density as $l_0 = 1/(\sqrt{2}n_\mathrm{ref}\,\pi d^2)$. As a reference value of the DF, we choose $f_\mathrm{ref} = n_\mathrm{ref}/u_\mathrm{T}^3$.

2.2 Phenomenological momentum and heat transfer laws

The Chapman–Enskog (CE) method allows deriving a linear relation between the viscous stress tensor and the shear rate tensor

$$S_{ij} = \frac{1}{2}\left(\frac{\partial u_i}{\partial x_j} + \frac{\partial u_j}{\partial x_i}\right) - \frac{1}{3}\,\delta_{ij}\,\frac{\partial u_r}{\partial r}\,,$$

and between the heat flux and the temperature gradient as follows:

$$\mathbf{p} = -2\mu\mathbf{S}\,, \tag{4}$$

$$\mathbf{q} = -\lambda\,\mathrm{grad}\,(T)\,. \tag{5}$$

Here, λ and μ are the respective thermal conductivity and viscosity coefficients.

These relations are well known as Newton's and Fourier's laws and are phenomenological laws of momentum and heat transfer. However, their derivation within the CE method is based on the a priori hypothesis of local equilibrium, which may be too strong a limitation for a wide class of phenomena. Dropping the principle of local equilibrium in the framework of extended irreversible thermodynamics allows obtaining evolutionary equations for the heat flux and the viscous stress tensor that are applicable to the description of fast processes; in the case of slow phenomena, they reduce to the classic laws.

The following assumptions are made in the classic approach [39]: "...There are, as it were, two large equilibrium systems... with noncoinciding values of density, temperature, and so on, and the system under study is inserted between them, ...with the transfer processes occurring across the system.... Simplifying assumptions of the theory of transfer phenomena in gases [are that] (a)... a local equilibrium state is realized in each planar layer, ... (b)... having run a path l in any direction, ... the particles become part of the equilibrium thermal motion, but now in a new layer,... (c)... moving from layer to layer, the particles transfer not only themselves but also their characteristics: energy, momentum, and so on."

2.3 Example of anomalous relation between heat flux and temperature gradient

We show that, in a nonequilibrium system, heat transfer can occur differently than the classic one, namely, from a cold to a hot region. This can be the case if nonequilibrium DFs are defined at two close points of the region x_A and x_B ($x_A < x_B$).

For example, we can consider a sum of two Maxwellian functions:

$$f_A = f_M\left(n, \mathbf{u}_0 = \{-u_0, 0, 0\}, T_A^0\right) + f_M\left(n, \mathbf{u}_1 = \{u_0, 0, 0\}, T_A^1\right),$$

$$f_B = f_M\left(n, \mathbf{u}_0 = \{-u_0, 0, 0\}, T_B^0\right) + f_M\left(n, \mathbf{u}_1 = \{u_0, 0, 0\}, T_B^1\right).$$

The parameters of the Maxwell functions are as follows here: the particle number densities are the same and equal to n, and the velocity vectors $\mathbf{u}_0$ and $\mathbf{u}_1$ have equal absolute values, but opposite directions. The temperatures of the Maxwellians, T_A^0, T_A^1 and T_B^0, T_B^1, are chosen different, so as to ensure nonzero heat fluxes of the DFs f_A and f_B. The temperature values can be chosen arbitrarily, but additional conditions must be satisfied to obtain anomalous transfer, as we show below.

In terms of the quantities in (2) and dimensionless macroparameters, it is easy to determine the temperatures and heat fluxes at points x_A and x_B for the DFs f_A and f_B:

$$T_{A,B} = \frac{1}{2}\left(T_{A,B}^0 + T_{A,B}^1\right) + \frac{2}{3}u_0^2,$$

$$q_{A,B} = \frac{5}{2}nu_0\left(T_{A,B}^1 - T_{A,B}^0\right).$$

By fixing the temperatures such that $T_B^1 + T_B^0 > T_A^1 + T_A^0$, we have $T_B > T_A$ for the temperatures of the DFs f_A and f_B; for $u_0 > 0$ and $T_{A,B}^1 > T_{A,B}^0$, we also have positive heat fluxes $q_{A,B} > 0$. It hence follows that $q_A(T_B - T_A) > 0$ and $q_B(T_B - T_A) > 0$. In other words, the presence of such DFs at close points in the region can make anomalous heat transfer possible.

However, the DFs in the above example are not solutions of the kinetic equation, and no anomalous heat transfer occurs when the DFs are transposed. This example of two artificially selected functions is only an illustration of the anomalous relations that can exist between the heat flux and the temperature gradient; it shows that the relations between the signs of the heat flux and the temperature gradient can be arbitrary in the general case. Therefore, it seems important to determine whether anomalous transfer can be obtained as a result of solving specific problems based on the kinetic equation. We note that, in the considered case, the momentum transfer is nonclassical for any arrangement of the chosen DFs, because there is no change in velocity, and the component of the viscous stress tensor p_{xx} is nonvanishing.

3. Heat transfer in classical and nonclassical cases

Although conditions (4) and (5) are obtained under the assumption of local equilibrium, they can be satisfied qualitatively and sometimes even quantitatively in strongly nonequilibrium flows. This can be demonstrated, for example, by solving the well-known problem of heat transfer between plates heated differently.

3.1 Classical heat transfer problem

The one-dimensional problem of heat transfer between two plates with fixed different surface temperatures is an example of a flow frequently used to test different models.

The classic problem setting is to find the temperature profile and the heat flux value between two plates separated by a distance L. In our calculation, the right plate has the temperatures $T_w = 4$, and the left, $T_w = 1$. The boundary conditions for particle reflection are assumed to be diffuse with full accommodation. The solutions in [40–42] demonstrate a correspondence between the temperature and heat flux in qualitative agreement with (5) in the entire range of Knudsen numbers $\mathrm{Kn} = l_0/L$ (Fig. 1) for molecules interacting by the hard-sphere law. The analytic solution presented in [43] using the Liu and Lees moment approximation [44] also shows a quantitative agreement with (5) for Maxwell molecules. This example is interesting in that qualitative agreement with Fourier's law is observed in this flow even at large Knudsen numbers, when the DF is strongly nonequilibrium: the heat flux is negative at all Knudsen numbers, i.e., is directed from the right (hot) plate to the left (cold) one.

However, flows are possible where Eqn (5) is fundamentally violated, e.g., where $q_x(\partial T/\partial x) > 0$ in the entire flow region or a part of it. One example of such a flow is the problem of heat transfer induced by nonequilibrium thermal reflection with the boundary conditions defined below, similar to the one considered above.

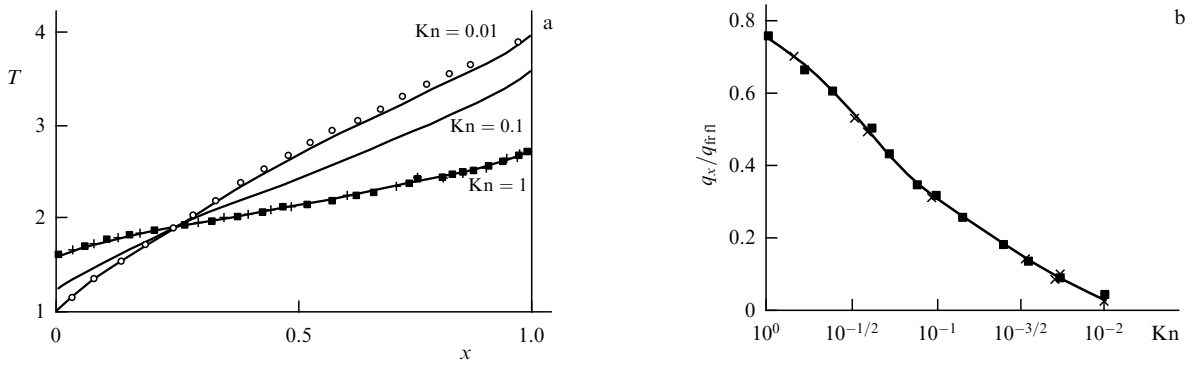

Figure 1. Classical heat transfer problem (with diffuse reflection). Left plate temperature $T_w = 1$, right plate temperature $T_w = 4$. (a) Temperature profiles T for different Knudsen numbers, (b) dependence of heat flux q_x on the Knudsen number, normalized to heat flux of free-molecule flow q_{frfl}.

3.2 Heat transfer problem with nonequilibrium reflection

We study heat transfer under special boundary conditions [45]. When modeling the processes of gas interaction with the surface, the DF or the scattering kernel of reflected particles is constructed by introducing parameters and accommodation coefficients so as to match the experimental data. In a rigorous formulation, the problem of describing the interaction of particles with a surface was formulated in terms of the theory of scattering kernels by Cercignani [46]; in this theory, the DF of reflected particles $f_r(\boldsymbol{\xi})$ is related to the DF of incident particles $f_i(\boldsymbol{\xi}')$ by an integral operator with the scattering kernel $R(\boldsymbol{\xi}' \to \boldsymbol{\xi})$,

$$\xi_n f_r(\boldsymbol{\xi}) = \int_{\xi_n'<0} |\xi_n'| R(\boldsymbol{\xi}' \to \boldsymbol{\xi}) f_i(\boldsymbol{\xi}')\, d\boldsymbol{\xi}', \quad \xi_n > 0, \qquad (6)$$

where $\boldsymbol{\xi}$ and $\boldsymbol{\xi}'$ are the respective velocity vectors of the reflected and incident molecules, and ξ_n and ξ_n' are the corresponding projections onto the outward normal to the surface. The scattering kernel $R(\boldsymbol{\xi}' \to \boldsymbol{\xi})$ must satisfy the conditions of:

— positivity

$$R(\boldsymbol{\xi}' \to \boldsymbol{\xi}) \geqslant 0, \quad \xi_n > 0, \quad \xi_n' < 0,$$

— normalization

$$\int_{\xi_n>0} R(\boldsymbol{\xi}' \to \boldsymbol{\xi})\, d\boldsymbol{\xi} = 1, \quad \xi_n' < 0,$$

— reciprocity

$$|\xi_n'| R(\boldsymbol{\xi}' \to \boldsymbol{\xi}) \exp[-\beta_w^2 \xi'^2] = |\xi_n| R(-\boldsymbol{\xi} \to -\boldsymbol{\xi}') \exp[-\beta_w^2 \xi^2],$$

Here, $\beta_w = \sqrt{m/(2k_B T_w)}$ and T_w is the surface temperature. The positivity condition guarantees the positivity of the DF of the reflected particles, and the normalization condition allows the impermeability condition to be satisfied. The reciprocity and normalization conditions and relation (6) imply that, if the DF of the incident particles $f_i(\boldsymbol{\xi}')$ is Maxwellian with a surface temperature T_w, then the DF of the reflected particles $f_r(\boldsymbol{\xi})$ is also Maxwellian with the temperature T_w; in other words, the boundary condition does not violate the equilibrium state of the gas near the surface (see [46] for the derivation of the reciprocity condition and its consequences).

Such a reflection condition can be called equilibrium. However, the reciprocity condition that is valid in the quasiequilibrium state of surface atoms can be violated in their nonequilibrium state, i.e., in the presence of nonequilibrium physicochemical processes on the surface that cause anisotropic excitation. The scattering kernels used in our study do not satisfy the reciprocity condition; they model reflection that we call nonequilibrium thermal reflection.

We briefly describe the results in [45]. As in the classical setup, we consider a stationary one-dimensional problem of heat transfer between infinite plates with different temperatures, located in the planes $x = \pm 1/2$, where x is the Cartesian coordinate normalized to L, perpendicular to the plates. On the plates, the impermeability condition $\int \xi_x f(x_{\pm 1/2}, \boldsymbol{\xi})\, d\boldsymbol{\xi} = 0$ is set. For the DF of reflected particles on one of the plates (at $x = -1/2$ in [45]), two variants of conditions are considered. The first variant corresponds to reflection with the ellipsoidal DF

$$f\left(-\frac{1}{2}, \boldsymbol{\xi}, \xi_x > 0\right) = n_l^- \left(\frac{1}{2\pi T_{xl}^-}\right)^{1/2} \frac{1}{2\pi T_{yzl}^-} \times \exp\left(-\frac{\xi_x^2}{2T_{xl}^-} - \frac{\xi_y^2 + \xi_z^2}{2T_{yzl}^-}\right), \qquad (7)$$

where the longitudinal temperature T_{xl}^- and the transverse temperature T_{yzl}^- are different. Here and hereafter, the subscript l denotes the values specified on the left plate, and the superscript $(-)$ denotes the parameters of the functions for $\xi_x > 0$.

In the second variant, the DF of the reflected particles is a superposition of Maxwellians with different parameters:

$$f\left(-\frac{1}{2}, \boldsymbol{\xi}, \xi_x > 0\right) = n_l^- \left[\alpha f_M(u_{0l}, T_l^-) + (1-\alpha) f_M(u_{1l}, T_l^-)\right]. \qquad (8)$$

The density n_l^- in (7) and (8) is determined from the impermeability condition. Diffuse reflection with full accommodation is assumed on the right plate. The dimensionless temperature of the right plate is equal to 1.

A consequence of the BE and the no-leakage boundary conditions on both plates is the zero value of the longitudinal velocity $u_x = 0$, and the constant values of the heat flux $q_x = \text{const}$ and the longitudinal component of the stress tensor $P_{xx} = \text{const}$. Because the velocity is zero, the energy flux and the heat flux coincide. We note that, although boundary condition (8) involves the velocity, the gas between the plates is at rest; boundary condition (8) is not a condition for the motion of the gas or the boundary, but corresponds to the process of emission of particles from the surface with a certain fixed velocity. Using the Liu and Lees two-sided distribution [45] in the free-molecular flow regime, we find the range of the parameters in conditions (7) and (8) that ensure anomalous heat transfer, with $q_x \partial T/\partial x > 0$. These regions are shown in gray in Figs 2 and 4a. Because the anomalous transfer regions are obtained in the free-molecular regime, obtaining the anomalous heat transfer for arbitrary Knudsen numbers requires numerical verification using the full BE.

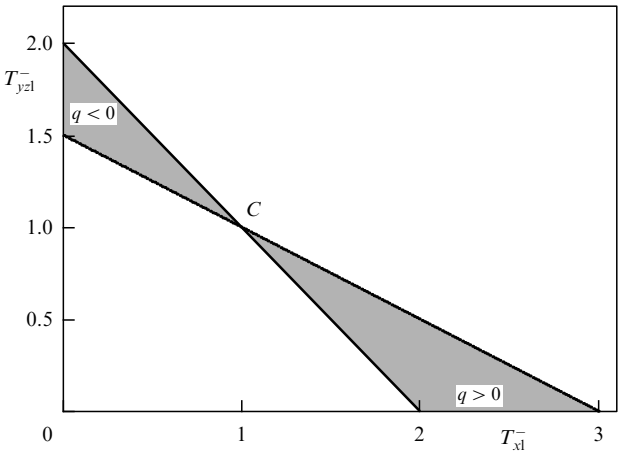

Figure 2. Anomalous transfer regions (shown in gray) of longitudinal, T_{xl}^-, and transverse, T_{yzl}^-, temperatures for boundary condition (7).

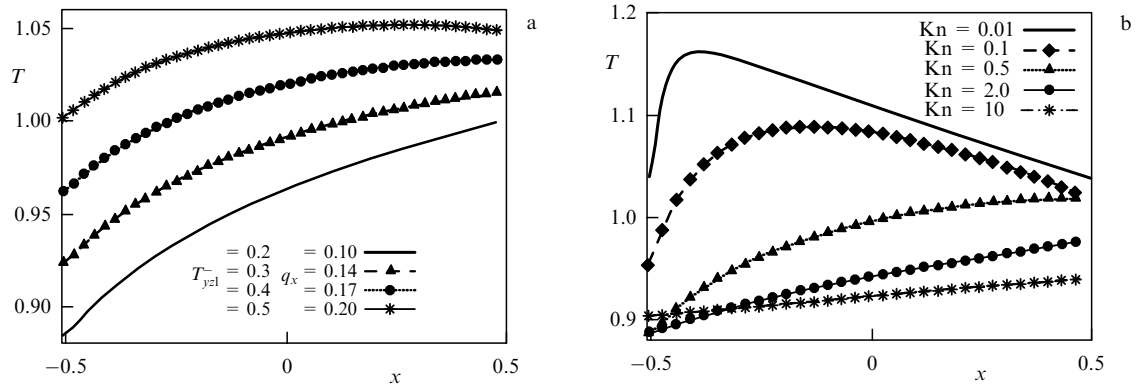

Figure 3. (a) Temperature profiles for boundary condition (7) with $T_{x1}^- = 2$, $0.2 \leqslant T_{yz1}^- \leqslant 0.5$, and Kn = 1, (b) temperature profiles at $T_{x1}^- = 2$ and $T_{yz1}^- = 0.2$ and different values of the Kn number.

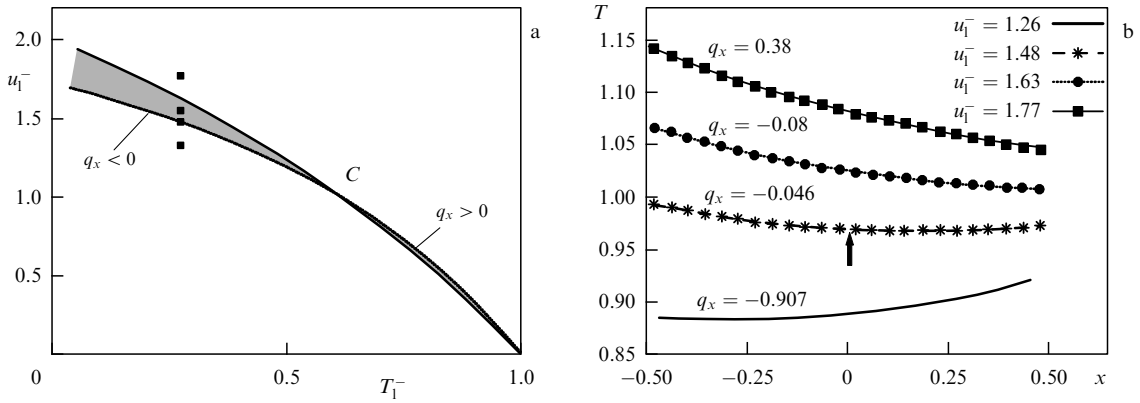

Figure 4. Results of heat transfer calculations for boundary condition (8). (a) Anomalous heat transfer regions of longitudinal velocity u_1^- and temperature T_1^- are shown in gray, (b) temperature profiles between plates (heat flux values are shown above curves).

The anomalous transport for the found parameter values in the boundary condition was confirmed by numerically solving the BE at arbitrary Knudsen numbers. In Figure 3a, we show the temperature profiles with boundary values $T_{x1}^- = 2$ and $0.2 \leqslant T_{yz1}^- \leqslant 0.5$ at Kn = 1. It is evident from the figure that, for $T_{yz1}^- < 0.5$, we have $q_x \partial T/\partial x > 0$ in the entire flow region, and at $T_{yz1}^- = 0.5$, the anomalous transport is observed in a part of the region. The effect of gas rarefaction is shown in Fig. 3b at $T_{x1}^- = 2$ and $T_{yz1}^- = 0.2$. As the Knudsen number decreases, the heat flux decreases, remaining positive. As x increases, a transition to classical heat transfer occurs, which is associated with the Maxwellianization of the DF. The size of the anomalous heat transfer zone remains of the order of the mean free path; the zone is located in the Knudsen layer near the left plate, which confirms the kinetic nature of the phenomenon. We emphasize that the anomalous behavior at small Knudsen numbers is observed only in a part of the region in the Knudsen layer (on the left).

For boundary conditions (8), the DF of the reflected particles is a superposition of two Maxwellians with the same temperature T_1^- but with different velocities. For $\alpha = 0$ and a nonzero longitudinal velocity component, the boundary condition has the form

$$f\left(-\frac{1}{2}, \xi, \xi_x > 0\right) = n_1^- f_M(u_1^-, T_1^-)\,.$$

The range of boundary condition parameters that lead to the violation of Fourier's relation for heat transfer is shown in Fig. 4a; as we can see, it is very narrow.

The results of calculations at Kn = 1 and $T_1^- = 0.273$ in the range $1.26 < u_1^- < 1.77$ (the values shown with squares in Fig. 4a) are presented in Fig. 4b. If the parameters u_1^- and T_1^- of boundary condition (8) fall into the anomalous transport region (the gray region $q_x < 0$ in Fig. 4a), then the numerical calculations confirm the fulfillment of the conditions $q_x(\mathrm{d}T/\mathrm{d}x) > 0$ for all x. For example, for $u_1^- = 1.63$ and $q_x = -0.08$, we have $\mathrm{d}T/\mathrm{d}x < 0$ in the entire region. If the values of u_1^- and T_1^- fall on the boundary of the region, the calculations demonstrate a decrease in the temperature gradient and the appearance of a local minimum inside the flow region: $u_1^- = 1.48$ and $q_x = -0.046$. The minimum temperature point is marked with an arrow in Fig. 4b. For the values of u_1^- and T_1^- that do not belong to the anomalous heat transfer region, the nature of the flow corresponds to classical heat transfer; for example, for $u_1^- = 1.26$ and $q_x = -0.907$, the temperature increases throughout the region, while for $u_1^- = 1.77$ and $q_x = 0.38$, the temperature decreases.

In [47], the occurrence of anomalous heat transfer in a one-dimensional flow in a region bounded by a membrane and a plate was demonstrated based on the Shakhov model equation [2]. The estimates obtained for the free-molecular regime are confirmed by calculations at various values of the Knudsen number.

4. Nonequilibrium flow with nonuniform relaxation

Relaxation problems are characteristic of kinetic theory when studying the transition from nonequilibrium to equilibrium states. In the traditional formulation of the problem of uniform relaxation, the DF is assumed to be independent of the physical space coordinates. At the initial instant, a nonequilibrium DF is specified and its transition to equilibrium over time is investigated. In a new class of problems, relaxation processes in space are described: the nonuniform relaxation problem (NRP) was proposed and named so in [48–50, 41]. In this problem, in a stationary one-dimensional case, a nonequilibrium DF with a mean supersonic velocity corresponding to a sufficiently large Mach number is maintained at the boundary of the region. The transition to the equilibrium DF downstream is investigated. Setting nonequilibrium boundary conditions leads to spatial nonuniformity of the macroparameters in the flow.

Unlike the heat transfer problem, where the mass flow rate is zero, the mass flow is large in the NRP. We note that, if an equilibrium DF is maintained downstream at the boundary, neither this DF nor any macroparameters change, but we are not interested in such a trivial case; we are considering nonequilibrium at the boundary.

The NRP involves a small parameter that allows expanding and obtaining analytic relations (for some molecular models) corresponding to nonclassical transfer. An important problem for the experimental verification of effects is to maintain stationary nonequilibrium boundary conditions, i.e., ensure that the DF relaxation at the boundary of the region is prevented. Modern technologies can ensure such processes, which allows us to harbor hope of confirming the effects discussed below. In Section 6 below, we specify the problems that ensure stationary maintenance of nonequilibrium at the boundary.

4.1 Nonuniform relaxation in supersonic regime throughout flow region

The NRP formulation is described in [50, 41] and is as follows: a half-space $x > 0$ is considered, a nonequilibrium DF $f(x = 0, \xi_x > 0) = F(\boldsymbol{\xi})$ is specified at the boundary $x = 0$, and the transition to equilibrium is investigated. During the relaxation of a given DF to supersonic equilibrium, the number of molecules with negative velocities is negligibly small, and the boundary condition at $x = +\infty$ is specified as

$$f(+\infty, \xi) = 0, \quad \forall\, \xi_x \leqslant 0\,.$$

The NRP solution for regimes with large Mach numbers at the input and with supersonic conditions at infinity is simpler than for other regimes, and it is in this formulation that anomalous transport relations were analytically identified for Maxwellian molecules governed by the BE and by the BGK model equation, which were then obtained in more general cases by numerical modeling. The results of the studies are described in [50–52, 41]. The DF fixed at the boundary for a supersonic mean velocity u_0 corresponding to the Mach number $\mathrm{M} > 3$ is localized in the velocity space region given by

$$\xi_x \in (u_0 - \Delta u_0, u_0 + \Delta u_0),\ |\xi_y| \in \Delta u_0,\ |\xi_z| \in \Delta u_0\,,$$

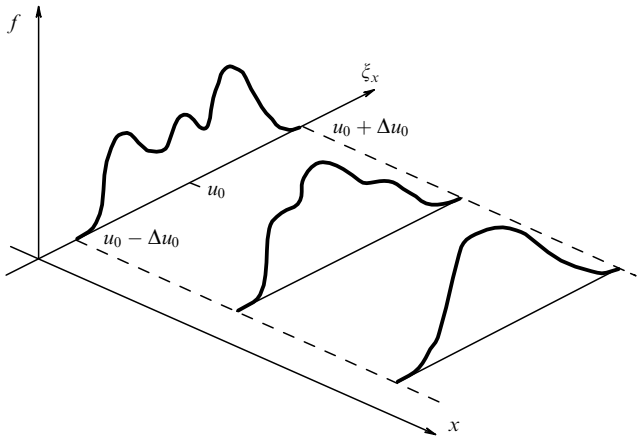

Figure 5. Schematic of spatial evolution of a DF in supersonic flow from a nonequilibrium distribution at the boundary to equilibrium distribution downstream.

where Δu_0 is a quantity of the order of several thermal velocities, and $u_0 - \Delta u_0 > 0$. Outside the interval $(u_0 - \Delta u_0, u_0 + \Delta u_0)$, the DF is assumed to be zero, which introduces only a small error, given the rapid decrease in the DF when molecular velocities deviate from the mean value. For clarity, in Fig. 5, we sketch the change in the DF in the solution region in the chosen setup.

In the one-dimensional case, the possibility of anomalous transport is demonstrated by series expanding the stationary kinetic equation in the neighborhood of the mean flow velocity in the small parameter $\alpha = (\xi_x - u)/u$, which has the same order of magnitude as the inverse Mach number $1/\mathrm{M}$ because $|\xi_x - u| \approx 3\sqrt{T}$ (we assume that the regime is realized in which $\alpha = \alpha(\xi_x) = (\xi_x - u_0)/u_0 < 1$, i.e., at a sufficiently large Mach number; here, u_0 is the mean velocity of the boundary DF). Also assuming a continuous dependence of the solution on the right-hand side of the equation, we obtain the corresponding approximations of the DF in α. For the NRP, the size of the spatial nonuniformity region is several mean free paths, and hence the characteristic Knudsen number of the problem is $\mathrm{Kn} \sim 1$ and the CE expansion is not valid.

The stationary one-dimensional BE has the form (with the collision integral used in the BGK form for simplicity)

$$\xi_x \frac{\partial f}{\partial x} = \frac{1}{\tau}\,(f_{\mathrm{M}} - f) = I(f)\,,$$

where f_{M} is the Maxwell function and τ is the relaxation time (in the simple case under consideration, it can be set constant, and, in a more general case, $1/\tau = p/\mu$, where p is the pressure and μ is the viscosity coefficient). It follows that the characteristic scale of the problem is determined by the quantity $u_0\tau$, equal in order of magnitude to the mean free path, which corresponds to $\mathrm{Kn} \sim 1$. We note that further reasoning is also valid for the full collision integral in the case of Maxwellian molecules. We divide both sides of the equation by the molecular velocity and, expanding $1/\xi_x = 1/u_0(1 + \alpha(\xi_x))$ in the small parameter α, we obtain

$$\frac{\partial f}{\partial x} = \frac{1}{u_0}\left(1 - \alpha + \ldots + (-1)^n \alpha^n + \ldots\right) I(f)\,. \tag{9}$$

By considering various approximations of the series in parentheses, we find various approximations of Eqn (9), the

DF, and the corresponding macroparameters. In the zeroth approximation,

$$\frac{\partial f^{(0)}}{\partial x} = \frac{1}{u_0\tau}\left(f_{\mathrm{M}}^{(0)} - f^{(0)}\right). \tag{10}$$

Here, $f_{\mathrm{M}}^{(0)}$ is the Maxwell function in the zeroth approximation, i.e., the one whose macroparameters are determined by $f^{(0)}$. This approximation corresponds to the equation of homogeneous relaxation, but the argument here is not time but a physical coordinate. We emphasize that, in contrast to the CE method, the zeroth approximation given by this expansion is a nonequilibrium function. Because the density, mean velocity, and temperature are spatially constant here, an analytic solution of (10) can easily be written, given that $F(\boldsymbol{\xi}) = f(x = 0, \xi_x > 0)$:

$$f^{(0)} = F(\xi)\exp\left(-\frac{x}{u_0\tau}\right) + f_{\mathrm{M}}^{(0)}\left(1 - \exp\left(-\frac{x}{u_0\tau}\right)\right).$$

Here, the components of the viscous stress and heat flux have finite values at the boundary and are vanishingly small downstream. The zeroth approximation for the DF differs from the exact expression by a quantity of the order of $O(\alpha)$, because this series is a Leibnitz series and the approximation error is determined by the first discarded term. The relation corresponding to the mass flux is satisfied exactly because $n = n_0$ and $u = u_0$. As the small parameter tends to zero, the solution reaches a relaxation solution with a single mean velocity u_0.

To find the relations between the macroparameters, we consider Eqn (9) in the second approximation:

$$\frac{\partial f^{(2)}}{\partial x} = \frac{1}{u_0}(1 - \alpha + \alpha^2) I\left(f^{(2)}\right). \tag{11}$$

Integrating (11) over the velocity space and taking the conservation laws into account, we obtain an equation for the density:

$$\frac{\mathrm{d}n^{(2)}}{\mathrm{d}x} = \frac{1}{u_0^3\tau}\int (\xi_x - u_0)^2\left(f_{\mathrm{M}}^{(2)} - f^{(2)}\right)\mathrm{d}\xi + O(\alpha^3).$$

Recalling that the collision integral is conservative, we find a relation between the density gradient and the viscous stress component p_{xx},

$$\frac{\mathrm{d}n^{(2)}}{\mathrm{d}x} = -\frac{1}{u_0^3\tau}\, p_{xx}^{(2)} + O(\alpha^3),$$

whence, taking the continuity equation into account, we find

$$\frac{\mathrm{d}u^{(2)}}{\mathrm{d}x} = \frac{u}{nu_0^3\tau}\, p_{xx}^{(2)} + O(\alpha^3). \tag{12}$$

Relation (12) is essentially a transfer equation and can be used to close the system of moment equations in the one-dimensional case for supersonic speeds with a high Mach number. The velocity gradient and the component of the nonequilibrium stress tensor are related here linearly, as in the well-known Newton–Stokes relations, but the signs on both sides are the same. We next derive a similar equation for heat transfer. For this, we integrate the right- and left-hand sides of (11) with the weight $(\xi_x - u)^2 + \xi_y^2 + \xi_z^2$, whence, taking into account that

$$\frac{\mathrm{d}n^{(2)}}{\mathrm{d}x}\, T^{(2)} = O(\alpha^2),$$

we obtain

$$\frac{\mathrm{d}T^{(2)}}{\mathrm{d}x} = \frac{2}{3nu_0^2\tau}\, q_x^{(2)} + O(\alpha^2). \tag{13}$$

It is evident that the signs of the temperature gradient and the heat flux, in contrast to Fourier's relation, are the same. This means that, to within α^2, transport equations (12) and (13) can be written as (omitting the superscripts for simplicity)

$$p_{xx} = \mu_U \frac{\mathrm{d}u_x}{\mathrm{d}x}, \tag{14}$$

$$q_x = \lambda_U \frac{\mathrm{d}T}{\mathrm{d}x}, \tag{15}$$

where $\mu_U = n_0 u_0^2\tau$ and $\lambda_U = 3n_0u_0^2\tau/2$.

In the case of the full BE with Maxwellian molecules (see [50]), these coefficients are given by

$$\mu_U = u_0^2 m\,\frac{(m/8K)^{1/2}}{6A},$$

$$\lambda_U = 3ku_0^2\,\frac{(m/8K)^{1/2}}{8A},$$

where m is the mass of the molecule and A and K are some constants. For other molecular models, it is impossible to obtain transport equations in closed form, and numerical simulation is used to solve the relaxation problem, although, by analogy with (14) and (15), one can try to write the same approximate relations here.

The established dependences were verified in various ways; in particular, in [53], sufficient conditions for the fulfillment of (14) and (15) were obtained. It was found that the anomalous transport conditions are satisfied at Mach numbers M_0 such that

$$\mathrm{M}_0 > \max(\mathrm{M}_1, \mathrm{M}_2), \quad \mathrm{M}_1 = 3\sqrt{\frac{3T_0}{5}}\,\sqrt[3]{\frac{u_0^2 C}{6|q_x|}},$$

$$\mathrm{M}_2 = \sqrt{\frac{3T_0}{5}}\,\sqrt[4]{\frac{54u_0^3 D}{|p_{xx}|}},\ C = \mathrm{const},\ D = \mathrm{const}.$$

Numerical calculations of the BE [51] for a monatomic gas with molecules interacting by the hard-sphere law for various nonequilibrium DFs at the boundary, specified as a superposition of two Maxwell functions $f_{\mathrm{M}}(n, u, T)$ (the values of the transverse velocity components being zero and omitted for brevity), confirmed the occurrence of anomalous transport. For some parameters of nonequilibrium boundary conditions, the downstream heating or cooling of the gas is accompanied by a significant change in temperature (by 40 to 50%) [52]. To confirm the results, the DSMC method was also used [54]. Figure 6 shows the profiles of the macroscopic parameters obtained when specifying the nonequilibrium DF $F(0, \boldsymbol{\xi}) = F_{\mathrm{M}}(1.5, 2.5, 1.0) + F_{\mathrm{M}}(0.5, 6.0, 1.0)$ in the boundary region, with the Mach number $\mathrm{M} = 2.32$ at the boundary.

Numerical experiments using the BGK model showed that the qualitative nature of the nonequilibrium (different

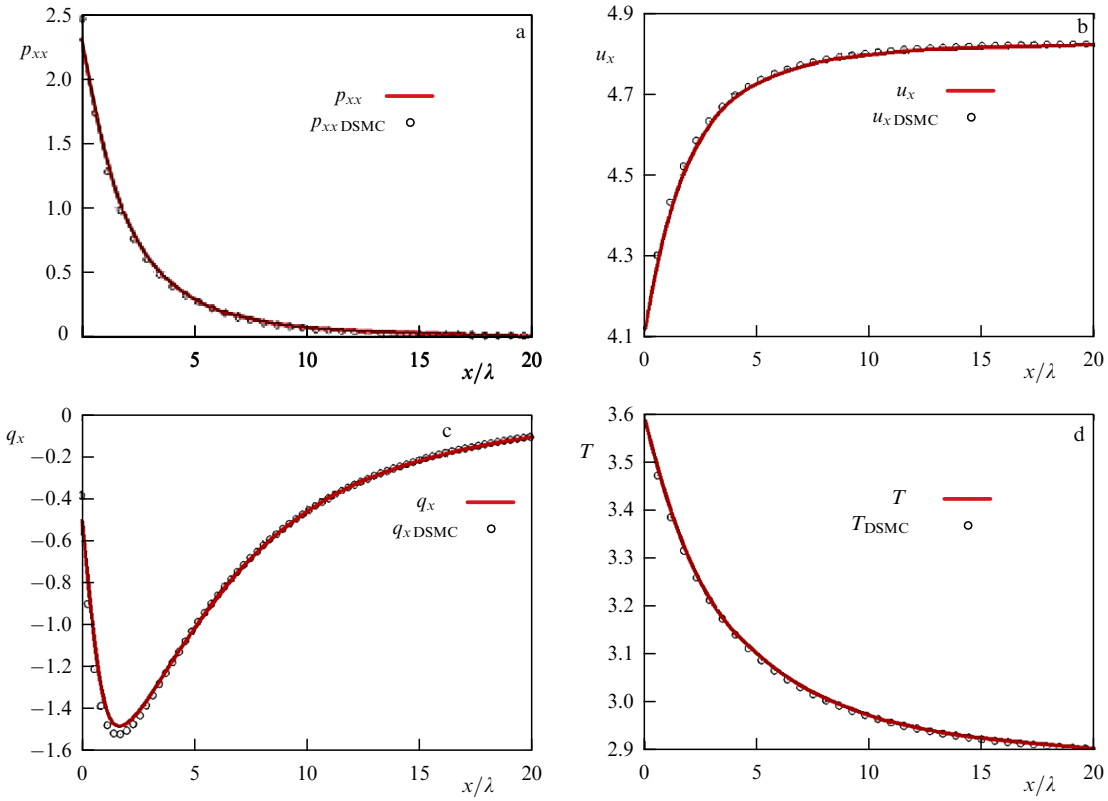

Figure 6. NRP calculation using DSMC and direct integration of BE. Profiles of (a) viscous stress tensor component p_{xx}, (b) velocity u_x, (c) heat flux q_x, and (d) temperature T. Circles: solution using DSMC method, solid lines: solution of BE.

from continuous) behavior of the heat flux components and the viscous stress tensor is affected only weakly by the type of collision operator.

4.2 Nonuniform relaxation in complex regimes

The nonequilibrium, fully supersonic flow in the above NRP is a simple open system described using kinetic methods. Such a nonequilibrium open system can be called a dissipative structure (a concept introduced by I. Prigogine to describe nonequilibrium open systems). The study of processes in such systems is interesting both from the theoretical standpoint and in connection with the emergence of new practical applications. At present, the best-known examples of dissipative structures are associated with a macroscopic approach. However, the analysis of nonclassical phenomena at a more detailed micro level using a kinetic description seems extremely important. For example, the NRP was studied in a linear formulation in [18], which allowed using the approximation by Hermite polynomials. Even in the linear case of a small deviation of the boundary conditions from equilibrium, anomalous transport is detected.

Numerical experiments with the NRP for mixtures of simple gases and molecular gases showed the emergence of regions with anomalous heat and stress transfer [55–56].

From a physical standpoint, it is of greater interest to study the NRP in the one-dimensional case for a simple one-component gas, but in regimes more complex than those discussed in the preceding section (see [51]).

The parameters of the equilibrium DF downstream — the density ρ_{eq}, velocity u_{eq}, and pressure p_{eq} — are determined from the conservation laws. At equilibrium, the heat flux and the components of the viscous stress tensor are zero, whence we obtain

$$\rho_{eq}u_{eq} = \rho_0 u_0 = C_0\,,$$
$$p_{eq} + \rho_{eq}u_{eq}^2 = p_0 + \rho_0 u_0^2 + p_{xx0} = C_1\,,$$
$$C_0\left[\frac{\gamma p_{eq}}{(\gamma-1)\rho_{eq}} + 0.5u_{eq}^2\right] = C_0\left[\frac{\gamma p_0}{(\gamma-1)\rho_0} + 0.5u_0^2 + \frac{p_{x0}}{\rho_0} + \frac{q_{x0}}{C_0}\right] = C_2, \qquad (16)$$

where ρ_0, u_0, p_0, q_{x0}, and $p_{x0} = P_{xx0} - p_0$ are the respective density, velocity, pressure, heat flux, and viscous stress tensor component at the boundary at $x = 0$, $\gamma = 5/3$ is the adiabatic exponent, and C_0, C_1, and C_2 are constants of motion. The solution of system (16) is

$$u_{eq} = \frac{\gamma C_1}{(\gamma+1)C_0} \pm \sqrt{\left(\frac{\gamma C_1}{(\gamma+1)C_0}\right)^2 - \frac{2(\gamma-1)C_2}{(\gamma+1)C_0}}, \qquad (17)$$

$$p_{eq} = C_1 - C_0 u_{eq}\,.$$

If the expression in the radicand in (17) and p_{eq} are nonnegative, then two equilibrium solutions exist for the macroscopic parameters set at the boundary $x = 0$. These two solutions satisfy the Rankine–Hugoniot relations: one corresponds to the subsonic and the other to the supersonic regime. The presence of two equilibrium regimes allows considering different formulations of this problem. We emphasize the similarity with and difference from a simpler, well-known formulation of the shock wave problem.

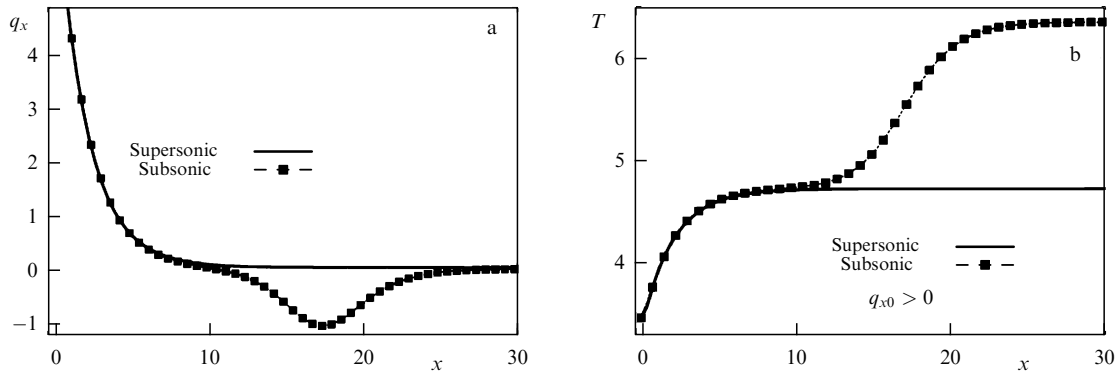

Figure 7. Profiles of macroparameters in NRP with subsonic and supersonic boundary conditions at output for $q_{x0} > 0$: (a) heat flux q_x, (b) temperature T.

We consider the case where the velocity u_0, determined by the DF specified at $x = 0$, is supersonic. If the DF $f(x = 0, \boldsymbol{\xi})$ is equilibrium, then supersonic solution (16) corresponds to a uniform flow homogeneous in space with the parameters $u_{\text{eq}} = u_0$, $\rho_{\text{eq}} = \rho_0$, and $p_{\text{eq}} = p_0$. The second solution implements the subsonic regime at $x_{\text{eq}} = x_\infty$ with the parameters $u_{\text{eq}} = [u_0(\gamma - 1) + 2\gamma p_0/C_0]/(\gamma + 1)$, $\rho_{\text{eq}} = C_0/u_{\text{eq}}$, and $p_{\text{eq}} = C_1 - C_0 u_{\text{eq}}$ and represents a shock wave profile.

If the DF at the boundary is chosen as a nonequilibrium one, then the macroscopic parameters at $x_{\text{eq}} = x_\infty$ for the supersonic solution differ from ρ_0, u_0, and p_0, and some new solution arises that describes the transition to equilibrium. As shown by numerical experiments, this solution has a particular kinetic behavior, and the relations of the viscous stress tensor components and the heat flux to the velocity and temperature gradients differ significantly from those adopted in the continuum modes of the Stokes (Newton) and Fourier laws.

Formulas (16) and (17) relate the boundary conditions at the right end of the downstream range to the flow parameters at the input at $x = 0$. Moreover, the values of the equilibrium macroscopic parameters at $x_{\text{eq}} = x_\infty$ for an arbitrary nonequilibrium DF at $x = 0$ can only be found in the course of solving the problem, because the DF at $\xi_x < 0$, which is necessary for calculating the integrals over the entire velocity space to determine the macroscopic parameters ρ_0, u_0, p_0, q_{x0}, and p_{xx0} at the input, is a priori unknown.

Analysis of the NRP in the supersonic case with a nonequilibrium boundary DF corresponding to moderate values of the Mach number (M < 3) [51] and taken to be a superposition of two Maxwellians, $f(\boldsymbol{\xi}) = f_{\text{M}}(n_1, u_1, T_1) + f_{\text{M}}(n_2, u_2, T_2)$ also showed the possibility of anomalous transport effects. At moderate Mach numbers, the boundary DF at infinity can no longer be equal to zero for negative velocities, and the parameters of the equilibrium DF are determined from relations (16) and (17) in the process of solving the problem. Numerous examples of numerical solutions have shown the formation of anomalous regions at moderate supersonic regimes of the boundary DF.

We consider the problem with nonequilibrium supersonic boundary conditions at the input and with a subsonic condition at the output. The problem statement is similar to the shock structure problem. The difference is that the conditions at the output (ρ_{eq}, u_{eq}, and p_{eq}) are determined by the values of ρ_0, u_0, p_0, q_{x0}, and p_{xx0} in (17) in the course of solving using the subsonic solution. A shock transition is realized in this case. However, in a narrow region near the boundary, an anomalous behavior of nonequilibrium moments is observed. It is interesting to note that, near the boundary, relaxation to equilibrium with supersonic parameters occurs, followed by a shock transition to subsonic flow; in other words, a transition to the supersonic branch occurs first, and only then, to the subsonic branch.

It turns out that the shock wave intensity increases at $q_{x0} < 0$ and decreases at $q_{x0} > 0$. Therefore, the nonequilibrium condition at the boundary can change the intensity of the shock transition. The anomalous behavior of the nonequilibrium moments is preserved in the region near the input, where the solution tends to a supersonic equilibrium flow. In the region of the shock transition, the anomalous behavior of the nonequilibrium moments is absent, because $p_{xx}\,\mathrm{d}u/\mathrm{d}x < 0$ and $q_x\,\mathrm{d}T/\mathrm{d}x < 0$ there. The profiles of heat fluxes and temperatures under subsonic and supersonic conditions and the same nonequilibrium DF at the input, corresponding to M = 1.5, are shown in Fig. 7 for $q_{x0} > 0$.

Unlike the supersonic boundary condition at the input, the solution in the case of the subsonic condition depends on the continuation of the DF at $x = 0$ to the region of negative velocities at the initial instant. Therefore, the stationary solution is not unique, and this formulation of the problem requires a special analysis.

In the multidimensional case, the heat transfer anomaly is defined as $(\mathbf{q}\nabla T) > 0$ (meaning that the projection of the heat flux vector onto the direction of the temperature gradient vector is positive).

The study of a two-dimensional supersonic jet flow from a slit into a vacuum with nonequilibrium boundary conditions at the input shows the occurrence of regions with anomalous heat transfer. Identifying the anomaly of viscous stress transfer in the multidimensional case is more complicated, and was not carried out.

5. Identifying anomalous transfer in flow past bodies

In this and the next sections, we present the results of modeling more complex (two-dimensional) flows where regions of nonclassical transfer are detected. Regimes are studied in a wide range of the rarefaction parameter (Knudsen number) in both unbounded and bounded regions. Flows in bounded regions are interesting, because different variants of open systems can be studied there.

In studying supersonic rarefied gas flows past a body, attention is focused on the neighborhood behind the body,

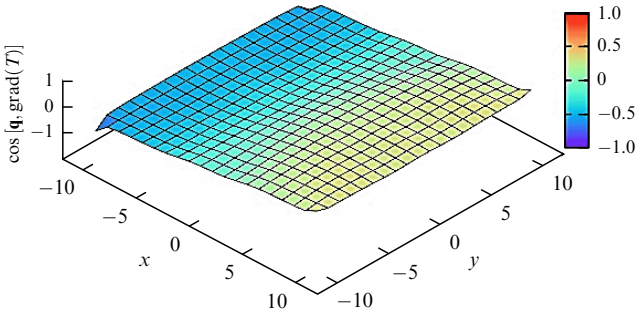

Figure 8. Cosine field of angle between heat flux and temperature gradient vectors. Position of plate center is $x = 0$, $y = 0$.

where a nonequilibrium distribution forms, which then approaches the equilibrium one further downstream. We can more or less assume that the flow in this region corresponds to that in the nonuniform relaxation problem.

Let us consider the classic problem of supersonic flow past an infinite planar plate (extended along the z-axis) of zero thickness and dimensionless length $L = 1$, located at $-0.5 < x < 0.5$, $y = 0$. In [57–60], this two-dimensional flow was studied in sufficient detail numerically by solving the BE with a full or model collision integral and the DSMC method, but the heat fluxes were not investigated. A detailed study [61] of the behavior of the heat flux and temperature gradient at Mach numbers $\mathrm{M} > 2$ and moderate Knudsen numbers using the solution to the full BE and the DSMC method demonstrates anomalous heat transfer behind the plate.

In this paper, the incident flow is described by the Maxwell DF with the dimensionless parameters $n = T = 1$ and $u = (\mathrm{M}\sqrt{\gamma T/2}, 0, 0)$, where $\gamma = 5/3$ is the adiabatic exponent. The interaction of molecules with the plate surface is assumed to be diffuse, with the plate temperature $T_{\mathrm{wall}} = 1$; the flow velocity at infinity and the rarefaction parameter are specified in the ranges $2 \leqslant \mathrm{M} \leqslant 4$ and $1 \leqslant \mathrm{Kn} \leqslant 10$.

The condition for anomalous heat transfer is the positivity of the cosine of the angle between the heat flux and temperature gradient vectors ($\cos\alpha = (\mathbf{q}\nabla T)/(|\mathbf{q}||\nabla T|) > 0$), which holds for $\alpha < 90^\circ$. In this case, the projection of the heat flux vector onto the temperature gradient direction, $q\cos\alpha$, and ∇T have the same direction, which corresponds to anomalous heat transfer. From Figure 8, which shows the $\cos\alpha$ field at $\mathrm{Kn} = 10$ at $\mathrm{M} = 3$, we can see a large region with nonclassical transfer behind the plate (shown in yellow).

Generalizing relations (14) and (15) between the heat flux and the temperature gradient, obtained in the one-dimensional NRP (Section 4), to the multidimensional case is apparently quite difficult, and this problem has not yet been solved. The assumption that similar equalities hold for each coordinate axis and can be used to close the moment equations is viable only at $\alpha = 0$ ($\cos\alpha = 1$). But the class of such flows is quite narrow, because the condition of anomalous heat transfer $\alpha < 90^\circ$ defines the region in which the projections of the vectors $\mathbf{q}$ and ∇T may not satisfy anomalous relations for all coordinate directions. In the multidimensional case, obtaining the conditions for a violation of the Newton–Stokes law for the viscous stress tensor components and shear rates is an even more difficult problem.

Therefore, it is of interest to analyze the behavior of the temperature T and the heat flux component q_x on the symmetry axis, where $q_y = 0$ and $\mathrm{d}T/\mathrm{d}y = 0$. From Fig. 9, which shows the q_x and T profiles at $\mathrm{Kn} = 1$ and different Mach numbers, it is evident that the components of the heat flux and temperature gradient are negative behind the plate, and the anomalous transfer becomes more pronounced as the Mach number increases.

6. Study of anomalous transport in flows with 'membrane-type' boundary conditions

Research associated with new technologies related to the production and use of membranes on the micro- and nanoscales is currently a promising field. It is becoming possible to study phenomena that were previously inaccessible to experimental analysis. A large number of studies are devoted to porous structures and membranes (see, e.g., [62–67]). Nanomechanical membranes seem to be especially important; they can be modeled and manufactured with a high degree of control and accuracy, primarily in terms of the accuracy of creating membrane pores, which then allows comparing theoretical and experimental results. For example, they are used in systems for determining mass and stress and creating an impermeable barrier layer. Such structures can be interesting due to their possible role in generating anomalous transport processes in regions bounded by membrane surfaces.

The approximation used to model the interaction of molecules with a porous medium requires dropping the no-flow condition. Under consideration are both simple boundary conditions, when molecules leaving the region do not interact (or interact weakly) with particles penetrat-

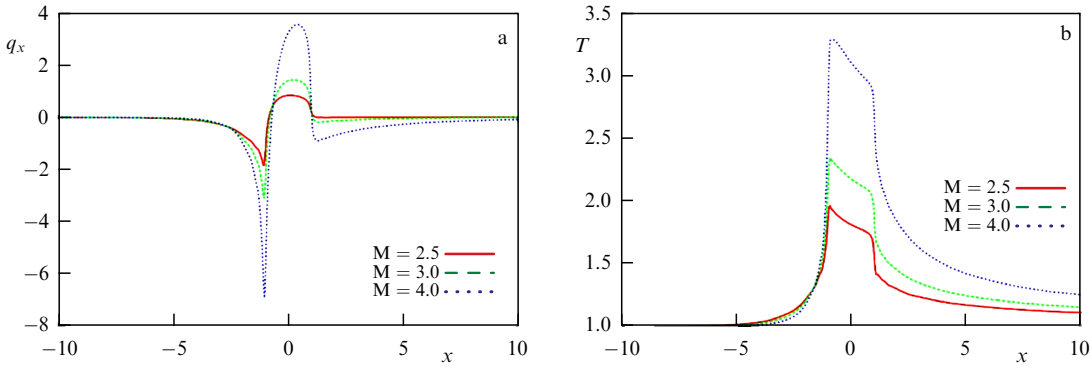

Figure 9. Flow past a plate at $\mathrm{Kn} = 1$ for different Mach numbers near symmetry line. Profiles (a) of heat flux component q_x and (b) of temperature T. Center of plate is located at $x = 0$.

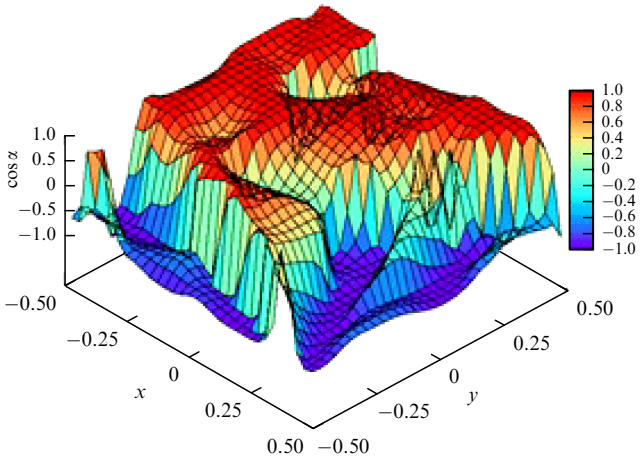

Figure 10. Simulation of a two-dimensional flow in a square domain with nonequilibrium boundary conditions: $\cos\alpha = (\nabla T, \mathbf{q})/(|\nabla T||\mathbf{q}|)$, $\mathrm{Kn} = 1$. Classical heat transfer corresponds to $\cos\alpha = -1$.

ing into the region, and more realistic 'membrane-type' conditions, which take reflection from membrane pores and the probability of percolation through a porous medium into account [68].

As an example of a flow with a simple boundary condition, we present the results of the numerical modeling of a two-dimensional steady planar flow in the square region $-0.5 \leqslant x \leqslant 0.5$, $-0.5 \leqslant y \leqslant 0.5$ bounded by membranes. At the boundaries of the region, i.e., on each side of the square, the DF is specified by the velocities of the incoming molecules, which can be either equilibrium or nonequilibrium, while the molecules reaching the surface from inside the region are assumed to be absorbed by the membrane and to not affect the distribution of the molecules entering the region [69]. The nonequilibrium DF is specified as a superposition of two Maxwellians with different parameters.

In Figure 10, where we plot $\cos\alpha = (\nabla T, \mathbf{q})/(|\nabla T||\mathbf{q}|)$ for the flow inside the region at $\mathrm{Kn} = 1$, we can see anomalous heat transfer ($\cos\alpha > 0$). Numerical experiments show that, as the Knudsen number decreases, the anomalous heat transfer zones narrow and localize near the boundaries of the region; for large values of the Knudsen number, they extend almost to the entire region.

We consider modeling more realistic 'membrane-type' boundary conditions using two variants of the interaction of molecules with membrane pores [70].

An infinitely thin membrane. In this case, the surface contains multiple pores. If a gas molecule enters a pore, it passes through the membrane without changing its velocity; otherwise, the molecule is reflected from the surface in accordance with the diffusion law. The ratio of the pore area to the total membrane area defines the permeability p_0, i.e., the probability of molecules passing through the membrane.

A finite-thickness membrane. In this case, the probability p_0 of a molecule entering a pore is determined in the same way as for an infinitely thin membrane. If a molecule enters a pore, it can either pass through without collisions with probability p_p or collide with the wall with probability $1 - p_\mathrm{p}$. A natural assumption is that the probability p_p depends on the molecular velocity and increases with the ratio of the normal velocity component ξ_n^2 to the tangential one ξ_τ^2 (normal and tangential to the membrane surface). The p_p dependences are considered in the form

$$p_\mathrm{p} = \sqrt{\frac{\xi_\mathrm{n}^2}{\xi_\mathrm{n}^2 + \xi_\tau^2}}, \tag{18}$$

$$p_\mathrm{p} = \frac{1}{\pi}\,(2\alpha - \sin 2\alpha)\,,$$
$$\begin{cases} \alpha = \arccos\left(\dfrac{H}{D}\,\dfrac{\xi_\tau}{\xi_\mathrm{n}}\right), & \dfrac{H}{D}\,\dfrac{\xi_\tau}{\xi_\mathrm{n}} < 1\,, \\ 0\,, & \dfrac{H}{D}\,\dfrac{\xi_\tau}{\xi_\mathrm{n}} \geqslant 1\,. \end{cases} \tag{19}$$

In (18), the probability p_p is equal to the cosine of the angle between the normal to the surface and the molecular velocity vector; in (19), p_p is the probability of a particle passing without collisions through a cylindrical pore of diameter D and a membrane of thickness H.

The effect of 'membrane-type' conditions on the flow is modeled by the following setups in one-dimensional geometry.

Setup 1. Flow through a flat membrane placed normally to the gas flow. The boundary condition for the DF is set at a sufficiently long distance from the membrane, where the effect of particles reflected from the membrane in the direction against the flow is negligible. The DF for the velocities of molecules entering the region in front of the membrane is $f = f_\mathrm{M}(n_0, u_0, T_0)$ with the dimensionless parameters $n_0 = T = 1$ and $u_0 = (\mathrm{M}\sqrt{\gamma T/2}, 0, 0)$. The membrane permeability is assumed to be sufficiently high, $p_0 > p_\mathrm{cr}$ (where p_cr is the critical value of permeability, depending on the Mach number of the incident flow and the membrane model), which guarantees the absence of a shock wave in front of the membrane due to the reverse flow of reflected particles.

From Fig. 11, which shows the profiles of the macroscopic parameters at different Mach numbers M and the permeability $p_0 = 0.9$ (the membrane placed at $x = 0$), it is clear that the region of anomalous heat and momentum transfer ($q_x \partial T/\partial x > 0$ and $p_{xx}\partial u_x/\partial x > 0$) appears behind the membrane for all considered values of the Mach number.

At $\mathrm{M} = 3$, the effect of the membrane thickness on the heat and momentum transfer for the incident flow can be seen in Fig. 12, which shows the macroscopic parameters for three membrane models: an infinitely thin and a finite-thickness one with the probability p_p in (18), $p_0 = 0.95$, and p_p in (19) at $H/D \leqslant 0.1$ and $p_0 = 0.9$.

It is evident from Fig. 12 that the width of the temperature profile in front of the membrane is larger for models with a finite-thickness membrane and is explained by a large number of molecules reflected from the membrane surface toward the incoming flow. In the flow behind the finite-thickness membrane, there is no anomalous transport with probability p_p in (19), unlike in the flow through an infinitely thin membrane and a membrane with p_p in (18). This difference can be explained by gas relaxation on the walls of membrane pores, due to which the gas state approaches equilibrium.

Setup 2. Flow passing through two infinitely thin membranes. In this case, $p_0 = 0.95$, the distance between the membranes is equal to two mean free paths, and the effective permeability of a system of two membranes is approximately 0.9. It is evident from Fig. 13 that, for all Mach numbers, there are regions of anomalous heat transfer and viscous stresses behind each of the membranes, ($q_x \partial T/\partial x > 0$ and $p_{xx}\,\partial u_x/\partial x > 0$).

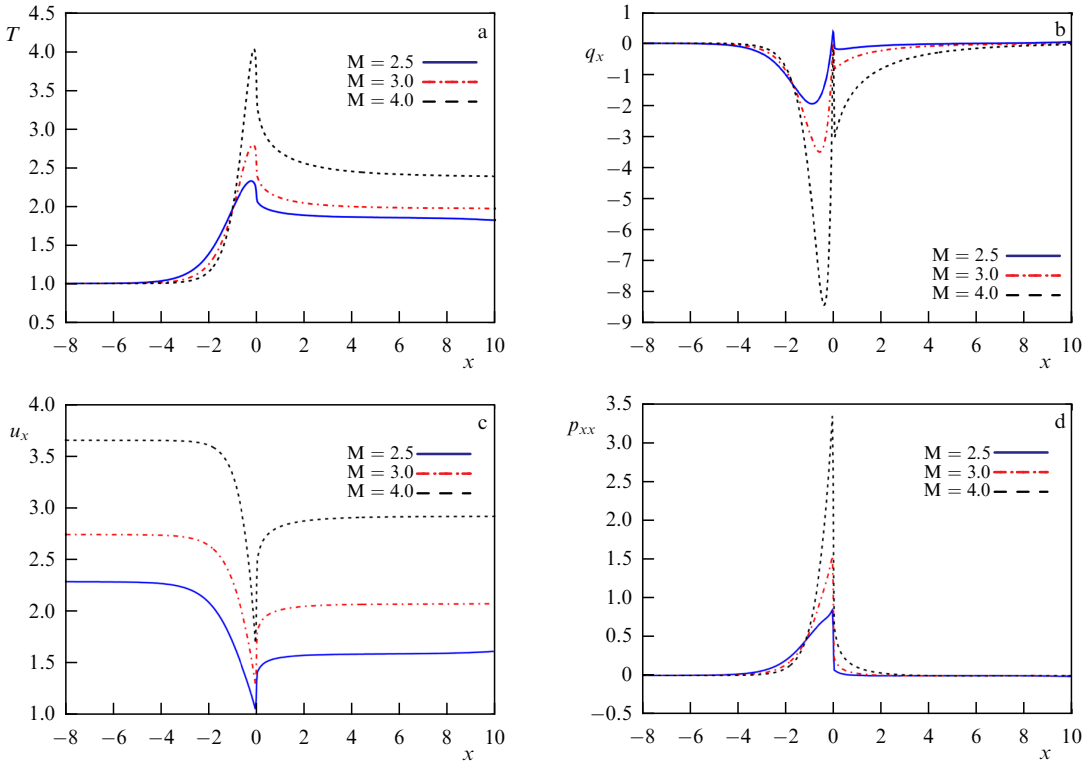

Figure 11. Flow through an infinitely thin membrane with permeability $p_0 = 0.9$ at Mach numbers M = 2.5, 3, and 4. Profiles of (a) temperature T, (b) heat flux component q_x, (c) velocity component u_x, (d) viscous stress tensor component p_{xx}.

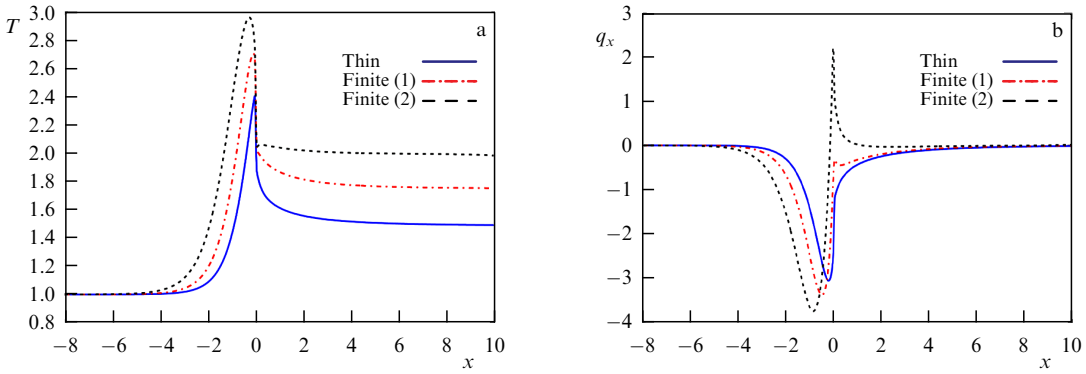

Figure 12. Comparison of different membrane models ($p_0 = 0.95$, M = 3.0): an infinitely thin membrane, a finite-thickness membrane, Eqn (18), a finite-thickness membrane, Eqn (19), at $H/D = 0.1$. Profiles of (a) temperature T, (b) heat flux component q_x.

Let us note that, in both considered formulations (a single membrane or a pair of membranes), the heat flux near the membrane and behind it is several times greater in absolute value than the heat flux calculated by Fourier's law.

An example of flow in two-dimensional geometry is given by supersonic flow through a grid formed by infinite (along the z-axis) cylindrical rods with a square cross section in the (x, y) plane and with the cross-section boundaries parallel to the axes, the central lines of the rods being equidistant and coplanar. The DF for the molecular velocities is the equilibrium one $f = f_{\mathrm{M}}(n_0, u_0, T_0)$ with the dimensionless parameters $n_0 = T = 1$ and $u_0 = (\mathrm{M}\sqrt{\gamma T/2}, 0, 0)$. The particle reflection from the grid surface is assumed to be diffuse with the surface temperature $T_w = 1$. The chosen square side d defines the characteristic scale of the problem. The solution is assumed to be periodic with the grid period $2H$, which is related to d via the expression for the geometric permeability of the grid, $p_0 = 1 - d/2H$. The optimal values $p_0 = 0.9$–0.95, as shown by numerical experiments, guarantee the absence of a shock wave in the reverse flow of particles reflected from the surfaces. Such a grid can be regarded as a highly permeable membrane (in reality, it must have high strength for use in experiments). When studying the nonequilibrium flow resulting from the interaction of a supersonic flow with the grid, reliable results are obtained from numerical experiments that involve directly solving the BE and the DSMC method; the results are given in [62]. Knudsen numbers Kn = 1–5 are considered at the Mach number M = 4 of the incoming flow.

The resulting anomalous transfer zone (at the Knudsen number Kn = 2) between the rods in the half-period region is shown in Fig. 14. As a result of the interaction of the supersonic flow with the plate or grid, a nonequilibrium flow arises, tending to equilibrium downstream. Figures 15 and 16 show how the DF relaxation occurs. Despite the two-humped shape of the DF in Fig. 15 (the points lying on the lower boundary in Fig. 14), nonclassical transfer in this region

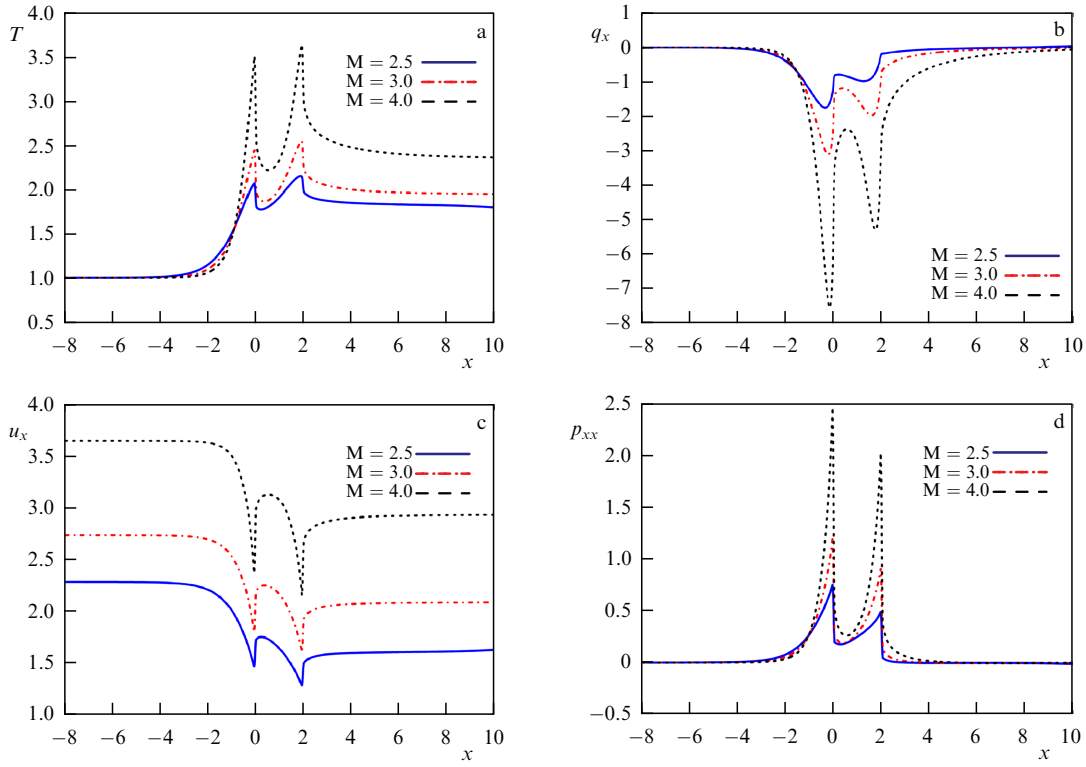

Figure 13. Flows for M = 2.5, 3, and 4, with membrane coordinates $x = 0$ and $x = 2$. Profiles of (a) temperature T, (b) heat flux component q_x, (c) velocity component u_x, (d) viscous stress tensor component p_{xx}.

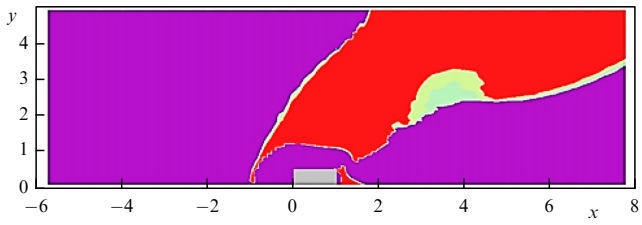

Figure 14. Flow through a grid, $\cos\alpha$ field at M = 4 and Kn = 2. Purple shows range of values $[-1, -0.1]$; red, $[0.1, 1]$; and other colors, $[-0.1, 0.1]$.

is practically absent (this question requires special consideration, but it is clear that even a strongly nonequilibrium distribution does not necessarily lead to anomalous transfer).

For some values of the y coordinate, there are zones of pronounced anomalous heat transfer. This is clearly seen at $y = 5.0$ in Fig. 14. The corresponding components of the temperature gradient and heat flux are negative in the region between the grid elements at $2 < x < 8$.

7. Consistency with second law of thermodynamics, nonequilibrium entropy, and prospects for experimental verification

The results obtained force us to address the problem of their consistency with the second law of thermodynamics. We note at once that the effects under consideration correspond to nonequilibrium flows, while the second law is formulated for equilibrium conditions. There are several essentially equivalent formulations of the second law. First, we quote the Clausius–Thomson formulation on the impossibility of spontaneous heat transfer from a cold body to a hot one. Clausius: "Heat cannot by itself pass from a cooler body to a hotter body" (Thomson's clarification: "It is impossible to transfer heat from a colder body to a hotter one without compensation, i.e., without changing the system itself and the bodies surrounding it"). The effects presented above do not contradict this formulation: for heat to flow from a cold zone to a hot one, a nonequilibrium distribution must be main-

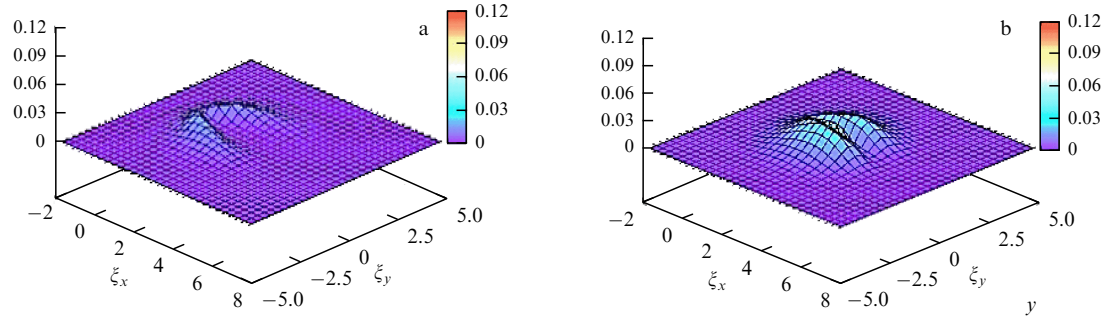

Figure 15. DF in the problem of flow through a grid on symmetry line behind grid elements at M = 4 and Kn = 2: $y = 0$; (a) $x = 1.5$ and (b) $x = 5.5$.

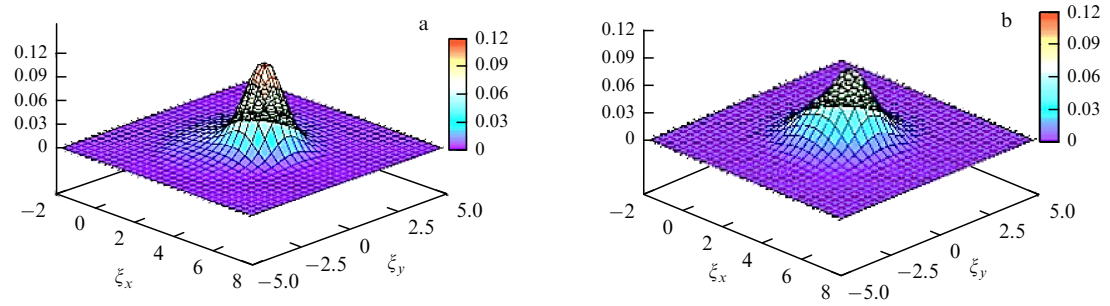

Figure 16. DF in the problem of flow through a grid on symmetry line between grid elements at M = 4 and Kn = 2: $y = 5.0$; (a) $x = 1.5$ and (b) $x = 5.5$.

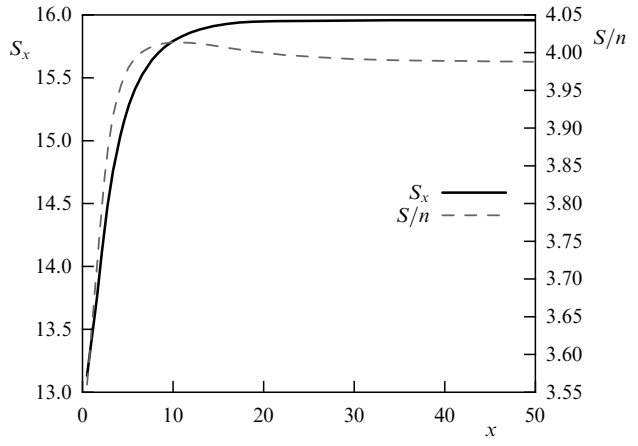

Figure 17. Profiles of reduced entropy S/n and entropy flux S_x in NRP.

tained, which requires expenditure of energy (and an increase in the total entropy).

Of importance in kinetic theory is Boltzmann's probabilistic formulation on the transition from a state with a lower statistical entropy to a state with a higher entropy in a closed system. The validity of this formulation, corresponding to the H-theorem, was verified directly in calculations in one- and two-dimensional flows. Therefore, in such a broader formulation, the second law preserves its original form, but attention should be paid to its correct interpretation for nonequilibrium states.

In Fig. 17, we show plots from [52], where an NRP was being solved. On the left boundary, for the molecules entering the region, the nonequilibrium DF is specified as a superposition of two Maxwellians in the form $F(0,\boldsymbol{\xi}) = F_{\mathrm{M}}(0.5, 1.0, 0.5) + F_{\mathrm{M}}(0.7, 5.0, 0.5)$. The profiles of the reduced entropy S/n (where n is the density) and the entropy flux S_x are shown. The entropy is defined here as the $-\mathrm{H}$ function with a Boltzmann constant factor; in accordance with (3), we then obtain $S = -k_{\mathrm{B}}H = -k_{\mathrm{B}}\int f \ln f \,\mathrm{d}\boldsymbol{\xi}$ and the entropy flux $S_x = -k_{\mathrm{B}}H_x = -k_{\mathrm{B}}\int \xi_x f \ln f \,\mathrm{d}\boldsymbol{\xi}$. The following remark is in order. In kinetic theory and in statistical physics, the concept of entropy is applied to arbitrary, not only equilibrium, states. We follow the traditional definition of entropy in physics. For example, in [71, p. 43], it is defined as the corresponding sum, and in [72, p. 67], as an integral (similar to that given above, but the integration is carried out in [72] over the phase space, while we integrate only over velocities, whence a dependence $S(x)$). The H-function (negentropy) is defined in (3), where the DF moments are introduced. When passing to a continuous medium with an equilibrium DF, the statistically defined entropy goes over into the known expression for gasdynamic entropy up to a factor given by density. At infinity on the right in Fig. 17, the reduced entropy S/n asymptotically tends to the equilibrium gasdynamic entropy.

The behavior of the above quantities confirms the fulfillment of the H-theorem. In the one-dimensional stationary case, this means a monotonic positive gradient of the entropy flux S_x, i.e., $S_{x\,\mathrm{output}} \geqslant S_{x\,\mathrm{input}}$, while the behavior of S itself and the reduced entropy S/n can be more complex (see Fig. 17).

In the multidimensional case, as can be easily shown, the fulfillment of the H-theorem corresponds to the condition $\operatorname{div}\mathbf{S} \geqslant 0$, where $\mathbf{S} = -k_{\mathrm{B}}\mathbf{H} = -k_{\mathrm{B}}\int \boldsymbol{\xi} f \ln f \,\mathrm{d}\boldsymbol{\xi}$ is the entropy flux. The numerical experiments in two-dimensional geometry for the problem of jet outflow with a nonequilibrium boundary condition confirm the fulfillment of this condition.

We conclude that nonequilibrium flows have been found (theoretically so far) in which heat transfer from a cold region to a hot region can occur on the mean free path scale. Our results require experimental verification, but the experiments are difficult due to the need to create stationary nonequilibrium and other boundary conditions capable of generating anomalous transfer.

In principle, the problem of creating nonequilibrium distributions constantly maintained in a spatial region can be solved in various ways. Obtaining some nonequilibrium function either in the region behind the body when a supersonic flow passes around it or when passing through a membrane seems realistic, as was demonstrated by the above calculations. It is also possible to use new modern technologies, so-called optical lattices (see, e.g., [73, 74]); the possibility of such an approach was confirmed by our numerical modeling in [52].

Recently, specific discussions of experimental verification of the effects under study have begun. Nonequilibrium distributions can be created in flows behind membranes. The desired permeability range is $p_0 = 0.9$–0.95, which actually corresponds to grids (nets). Figure 18 shows the basic setup of the experiment; this experimental test is planned to be implemented at the University of Marseille under the supervision of Dr. P. Perrier.

Two factors are important in the experiment: the creation of the necessary nonequilibrium and the diagnostic method. The first factor is implemented as a membrane located behind the nozzle, which produces a supersonic flow of rarefied gas. The electron beam fluorescence method can be used to determine the particle velocity distribution. In fact, it suffices to determine the nonequilibrium distribution and calculate the temperature and hence the heat flux at only one point

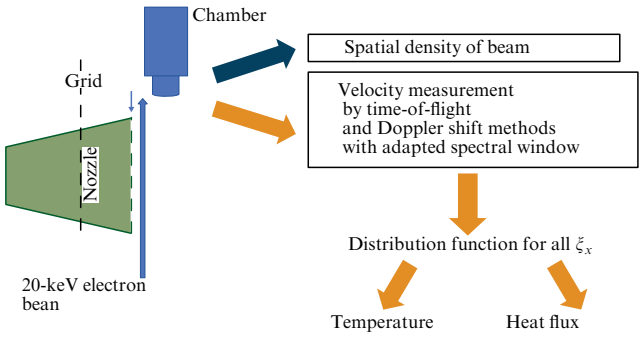

Figure 18. Schematic diagram of the experimental setup (a supersonic nozzle is shown on the left, a net (grid) is located immediately behind it; next, the incoming electron beam and a chamber are indicated, which allow detecting high particle velocities; DF can be determined, e.g., using Doppler effect).

behind the membrane (net). Because the downstream distribution is equilibrium, the heat flux there is zero, and the temperature can be measured using, for instance, a conventional thermometer.

The Clausius–Thomson formulation can be adjusted, because it is permissible to imagine natural phenomena with nonequilibrium states for which heat transfer from a cold region to a hot one is possible. The discovery of natural phenomena with these effects would mean that heat transfer from cold zones to hot ones is possible in nonequilibrium flows, and hence the formulation of the second law can be extended. We note that nonequilibrium states must be maintained by 'pumping' energy and negentropy (under normal conditions, spontaneously arising nonequilibrium relaxes to equilibrium in a very short time: the relaxation time in air is $\sim 10^{-9}$ s). Objects in terrestrial or cosmic conditions can act as natural phenomena where the indicated effects of nonclassical transfer are feasible. It is possible that these nonequilibrium states can be detected in highly nonequilibrium wakes and jets, in flows behind grids and thin membranes, in flows around descending spacecraft (in the bottom region behind the body, where a rarefied zone is formed), in upper layers of the atmosphere, and in astrophysical processes where particles have a long mean free path.

Nonequilibrium gas flows are currently of great importance and are relevant to virtually all areas of modern industry. Many technological applications can be named, including liquid microdrives for active control of aerodynamic flows, vacuum generators, flow and temperature microsensors, pressure gauges, microgas analyzers, and microheat exchangers for cooling electronic components or for thermal control of chemical processes and porous media. Therefore, the topic under consideration, in addition to purely physical interest, can also be promising in terms of applications, e.g., in creating new microdevices (in particular, microrefrigerators). When discussing the applied possibilities, it is useful to recall the history of the discovery and application of the above-mentioned effect of thermal transpiration, which took many years to develop from theory to applications.

In addition to the foregoing, we note modern studies (see, e.g., [75]) where various Maxwell demon schemes are implemented. Arguably, the creation of nonequilibrium distributions of molecules with the properties required for the described effects is not a more complex problem.

8. Conclusions

We outlined the results and problems associated with new effects of heat transfer and viscous stresses in gaseous media for highly nonequilibrium flows. Violation of the classical transfer conditions of the NS theory has long been detected in the framework of the continuous medium approximation. But, for microscopic scales of the order of the mean free path of molecules, such phenomena have begun to be noted relatively recently, and currently require detailed consideration due to the importance of studying nonequilibrium processes.

We have presented generalizations of the results, obtained both by ourselves and other authors, on nonclassical anomalous transport, i.e., relations between the heat flux and the temperature gradient and relations between the viscous stress tensor and the shear rate tensor, which are incompatible with the respective Fourier and Newton–Stokes laws. An important point is that the discovered anomalous relations lead to fundamental changes in the physical process, including heat and momentum transfers in the direction of increasing temperature and velocity.

The emergence of anomalous transfer regions is demonstrated for supersonic and hypersonic flows with nonequilibrium boundary conditions in a one-dimensional formulation (in the NRP), where the possibility of obtaining fundamentally new relations between dissipative flows and gradients of the corresponding quantities is also confirmed analytically in the considered modes.

Nonconventional heat transfer was modeled and numerically verified based on calculations of the full BE in the problem of heat transfer under nonequilibrium thermal reflection, in flows with complex boundary conditions that reproduce the characteristics of molecular flows passing through membrane pores. Anomalous transfer zones were observed numerically (by directly solving the BE and by the DSMC method) in flows around a planar plate with standard boundary conditions and in the passage of a supersonic flow through a grid.

In one-dimensional flows, the anomalous zones were generated by special nonequilibrium boundary conditions, which required some additional factors, but, importantly, in flows behind the plate and flows through the grid, the flows entering the region were in equilibrium. Such flows are widespread, and the obtained nonequilibrium state can serve as a condition for experimental verification.

We have discussed the possibilities of experimental tests and outlined the corresponding setup. Potentially possible manifestations of such effects in various natural phenomena are also considered. The discovered effects of nonclassical transport may also be important in future applications.

References

1. Osipov A I, Uvarov A V *Sov. Phys. Usp.* **35** 903 (1992); *Usp. Fiz. Nauk* **162** (11) 1 (1992)
2. Sobolev S L *Phys. Usp.* **40** 1043 (1997); *Usp. Fiz. Nauk* **167** 1095 (1997)
3. Grad H "Principles of the kinetic theory of gases," in *Thermodynamik der Gase* (Handbuch der Physik, Vol. 12, Encyclopedia of Physics, Vol. 3, Ed. S Flügge) (Berlin: Springer, 1958) p. 205; Translated into Russian: in *Termodinamika Gazov* (Moscow: Mashinostroenie, 1970) p. 5–109
4. Alam M, Mahajan A, Shivanna D *J. Fluid Mech.* **782** 99 (2015)
5. Maxwell J C *Philos. Trans. R. Soc. London* **170** 231 (1879)
6. Reynolds O *Philos. Trans. R. Soc. London* **170** 727 (1879)

7. Knudsen M *Ann. Physik* **336** 205 (1909)
8. Akhlaghi H, Roohi E *J. Phys. Conf. Ser.* **362** 012045 (2012)
9. Akhlaghi H, Roohi E, Stefanov S *Phys. Rep.* **997** 1 (2023)
10. Kryukov A P et al. *Phys. Usp.* **64** 109 (2021); *Usp. Fiz. Nauk* **191** 113 (2021)
11. Holway L H (Jr.) *Phys. Fluids* **8** 1905 (1965)
12. Yen S-M *Phys. Fluids* **9** 1417 (1966)
13. Salwen H, Grosch C E, Ziering S *Phys. Fluids* **7** 180 (1964)
14. Kogan M N *Rarefied Gas Dynamics* (New York: Plenum Press, 1969); Translated from Russian: *Dinamika Razrezhennogo Gaza. Kineticheskaya Teoriya*. (Moscow: Nauka, 1967)
15. Timokhin M Yu et al. *Phys. Fluids* **27** 037101 (2015)
16. Myong R S *Phys. Fluids* **23** 012002 (2011)
17. Taheri P, Torrilhon M, Struchtrup H *Phys. Fluids* **21** 017102 (2009)
18. Ilyin O *J. Stat. Mech.* **2017** 053201 (2017)
19. Venugopal V, Praturi D S, Girimaji S S *J. Fluid Mech.* **864** 995 (2019)
20. Baranyai A, Evans D J, Daivis P J *Phys. Rev. A* **46** 7593 (1992)
21. Todd B D, Evans D J *J. Chem. Phys.* **103** 9804 (1995)
22. Todd B D, Evans D J *Phys. Rev. E* **55** 2800 (1997)
23. Wang Z, Bao L, Tong B *Phys. Fluids* **22** 126103 (2010)
24. Gu X-J, Emerson D R *J. Fluid Mech.* **636** 177 (2009)
25. Kovács R *Entropy* **21** 718 (2019)
26. Bishaev A M, Rykov V A *Izv. Akad. Nauk. SSSR. Mekh. Zhidk. Gaza* (3) 162 (1980)
27. Kogan M N, Galkin V S, Fridlender O G *Sov. Phys. Usp.* **19** 420 (1976); *Usp. Fiz. Nauk* **119** 111 (1976)
28. Zhdanov V M, Roldugin V I *Phys. Usp.* **41** 349 (1998); *Usp. Fiz. Nauk* **168** 407 (1998)
29. Zhdanov V M, Roldugin V I *J. Exp. Theor. Phys.* **82** 683 (1996); *Zh. Eksp. Teor. Fiz.* **109** 1267 (1996)
30. Waldmann L, Vestner H *Physica A* **80** 523 (1975)
31. Martyushev L M *Phys. Usp.* **64** 558 (2021); *Usp. Fiz. Nauk* **191** 586 (2021)
32. Kuščer I *Physica A* **133** 397 (1985)
33. Zhdanov V, Kagan Yu, Sazykin A *Sov. Phys. JETP* **15** 596 (1962); *Zh. Eksp. Teor. Fiz.* **42** 857 (1962)
34. Jou D, Casas-Vazquez J, Lebon G *Rep. Prog. Phys.* **51** 1105 (1988)
35. Müller I, Ruggeri T *Extended Thermodynamics* (Springer Tracts in Natural Philosophy, Vol. 37) (New York: Springer-Verlag, 1993) https://doi.org/10.1007/978-1-4684-0447-0
36. Kolobov V I et al. *J. Comput. Phys.* **223** 589 (2007)
37. Shakhov E M *Izv. Akad. Nauk SSSR. Mekh. Zhidk. Gaza* (1) 156 (1968)
38. Bhatnagar P L, Gross E P, Krook M *Phys. Rev.* **94** 511 (1954)
39. Kvasnikov I A *Molekulyarnaya Fizika* (Moscow: URSS, LIBROKOM, 2011)
40. Aristov V V, Ivanov M S, Cheremisin F G *USSR Comput. Math. Math. Phys.* **30** 193 (1990); *Zh. Vychisl. Matem. Matem. Fiz.* **30** 623 (1990)
41. Aristov V V *Direct Methods for Solving the Boltzmann Equation and Study of Nonequilibrium Flows* (Dordrecht: Kluwer Acad. Publ., 2001); Aristov V V *Direct Methods for Solving the Boltzmann Equation and Study of Nonequilibrium Flows* 2nd ed. (Dordrecht: Springer, 2012) https://doi.org/10.1007/978-94-010-0866-2
42. Ohwada T *Phys. Fluids* **8** 2153 (1996)
43. Bird G A *Molecular Gas Dynamics* (Oxford: Clarendon Press, 1976); Translated into Russian: *Molekulyarnaya Gazovaya Dinamika* (Moscow: Mir, 1981)
44. Liu C Y, Lees L, in *Rarefied Gas Dynamics. Proc. of the Second Intern. Symp. on Rarefied Gas Dynamics* (Ed. L Talbot) (New York: Academic Press, 1961)
45. Aristov V V, Zabelok S A, Frolova A A *Dokl. Phys.* **62** 149 (2017); *Dokl. Ross. Akad. Nauk* **473** 286 (2017)
46. Cercignani C *Theory and Application of the Boltzmann Equation* (Edinburgh: Scottish Academic Press, 1975)
47. Ilyin O V *Comput. Math. Math. Phys.* **63** 2297 (2023); *Zh. Vychisl. Matem. Matem. Fiz.* **63** 2016 (2023)
48. Aristov V V, in *Rarefied Gas Dynamics. Proc. of the 17th Intern. Symp. on Rarefied Gas Dynamics, July 8–14, 1990, Aachen, Germany* (Ed. A E Beylich) (Weinheim: VHC, 1991) p. 879
49. Aristov V V, in *Trudy Pervoi Rossiiskoi Natsional'noi Konf. po Teploobmenu, 21–25 Noyabrya 1994, Moscow, Russiya* (Proc. of the First Russian National Conf. on Heat Transfer, November 21–25, 1994, Moscow, Russia) Vol. 10, Ch. 2 (Moscow: MEI, 1994) p. 36
50. Aristov V V *Phys. Lett. A* **250** 354 (1998)
51. Aristov V V et al. *Comput. Math. Math. Phys.* **56** 854 (2016); *Zh. Vychisl. Matem. Matem. Fiz.* **56** 869 (2016)
52. Aristov V V, Frolova A A, Zabelok S A *Commun. Comput. Phys.* **11** 1334 (2012); *Zh. Vychisl. Matem. Matem. Fiz.* **56** 869 (2016)
53. Aristov V V, Panyashkin M V *Comput. Math. Math. Phys.* **51** 122 (2011); *Zh. Vychisl. Matem. Matem. Fiz.* **51** 131 (2011)
54. Ivanov M S, Markelov G N, Gimelshein S F *AIAA Paper* **98** 2669 (1998)
55. Aristov V V, Frolova A A, Zabelok S A *Europhys. Lett.* **88** 30012 (2009)
56. Aristov V V, Zabelok S A, Frolova A A *Matem. Modelir.* **21** (12) 59 (2009)
57. Bird G A *AIAA J.* **4** (1) 55 (1966)
58. Cheremisin F G *Sov. Phys. Dokl.* **18** 203 (1973); *Dokl. Akad. Nauk SSSR* **209** 811 (1973)
59. Aoki K, Kanba K, Takata S *Phys. Fluids* **9** 1144 (1997)
60. Abramov A A, Butkovskii A V, Buzykin O G *Phys. Fluids* **32** 087108 (2020)
61. Aristov V V, Voronich I V, Zabelok S A *Comput. Math. Math. Phys.* **63** 2306 (2023); *Zh. Vychisl. Matem. Matem. Fiz.* **63** 2025 (2023)
62. Mattia D et al. *Philos. Trans. R. Soc. A* **374** 20150035 (2016) https://doi.org/10.1098/rsta.2015.0035
63. Yoon H W, Cho Y H, Park H B *Philos. Trans. R. Soc. A* **374** 20150024 (2016) https://doi.org/10.1098/rsta.2015.0024
64. Wang L et al. *Nano Lett.* **17** 3081 (2017)
65. Lasseux D, Valdés Parada F J, Porter M L *J. Fluid Mech.* **805** 118 (2016)
66. Moghaddam R N, Jamiolahmady M *Fuel* **173** 298 (2016)
67. Borner A, Panerai F, Mansour N N *Int. J. Heat Mass Transfer* **106** 1318 (2017)
68. Aristov V V, Zabelok S A, Frolova A A *Modelirovanie Neravnovesnykh Struktur Kineticheskimi Metodami* (Modeling of Nonequilibrium Structures by Kinetic Methods) (Moscow: Fizmatkniga, 2017)
69. Aristov V V, Voronich I V, Zabelok S A *Phys. Fluids* **33** 012009 (2021)
70. Aristov V V, Voronich I V, Zabelok S A *Phys. Fluids* **31** 097106 (2019)
71. Landau L D, Lifshitz E M *Statistical Physics* Vol. 1 (Oxford: Pergamon Press, 1980); Translated from Russian: *Statisticheskaya Fizika* Ch. 1 (Moscow: Fizmatlit, 2002)
72. Klimontovich Yu L *Statistical Physics* (Chur: Harwood Acad. Publ., 1986); Translated from Russian: *Statisticheskaya Fizika* (Moscow: Nauka, 1982)
73. Barker P F, Shneider M N *Phys. Rev. A* **64** 033408 (2001)
74. Fulton R et al. *Nature Phys.* **2** 465 (2006)
75. Koski J V et al. *Phys. Rev. Lett.* **115** 260602 (2015)